

UNIVERSITÀ DEGLI STUDI DI PADOVA

Dipartimento di Fisica e Astronomia “Galileo Galilei”

Master Degree in Physics

Final Dissertation

Crystal and pattern formation for probes in contact
with a nonequilibrium system

Thesis supervisor

Prof. Marco Baiesi

Thesis co-supervisor

Prof. Christian Maes

Candidate

Tommaso Tonolo

Academic Year 2020/2021

Abstract

In this thesis we study a nonequilibrium model that displays interesting and unusual phenomena. The analysed system consists of multiple probes locally interacting with driven colloids and trapped in a toroidal geometry. The effective forces between the probes break the action-reaction principle and these interactions induce, under particular conditions, stability of a crystal pattern, in which the probes are equidistant. In this thesis we explore the thermodynamic limit of such a system. Sending both the number of probes and the length of the ring to infinity it is possible to analyse how a perturbation on a hypothetic infinite crystal configuration perturbs such a system.

Contents

Introduction	1
1 Theoretical background	5
1.1 Fokker-Planck equation	5
1.2 Langevin equation	10
2 The model	13
2.1 Stationary density	14
2.2 Driving-induced forces	21
3 Crystal pattern stability	25
4 Relaxation to the crystal pattern	31
4.1 The case with 2 and 3 probes	32
4.1.1 System of 2 probes	32
4.1.2 System of 3 probes	32
4.2 Dynamics as a Compound Poisson Process	33
4.3 Approximation of the elastic constants	36
4.3.1 Multi-probe initial conditions	40
4.3.2 Time-scales	42
4.3.3 A natural ansatz for the Poisson process' master equation	45
4.3.4 Contribution of all the elastic constants m_γ	48
5 Thermal stability	53
6 Thermodynamic limit	59
6.1 White noise	66
6.2 The damping law	69

Introduction

Every physical system can be described in two ways, by a microscopic or a macroscopic point of view. Let us consider for example a gas in a box. The physical system that describes the gas consists of an enormous number of interacting particles. In this sense the system can be described by the Newton equations: each particle has a defined position and velocity that depend on time. If we could solve these equations we would have a perfect knowledge of the evolution of each particle of the gas in time. But this is obviously not possible as usually, in Physics, systems are too complicated to be solved by the Newton equations and the single-particle dynamics is practically unpredictable. On the other hand, macroscopically, a gas can be described thermodynamically just by its temperature and pressure.

The two different interpretations of the (gas) system are equivalent, but their gap is very difficult to fill. And here Statistical Mechanics comes to our aid.

During the nineteenth century a new theory, a bridge between microscopic and macroscopic worlds, started to rise [5], [19]. One of the most important concepts of Statistical Mechanics is the definition of two different kind of states: the microstate and the macrostate. The former is described by Newtonian equations' dynamics, the latter by a small number of state functions like energy E , temperature T , pressure P and number of particles N .

Each microstate needs a huge amount of information in order to be described and in particular there is a very large number of microstates corresponding to the same macrostate. The goal of statistical mechanics is really to examine, instead of a single microstate, an ensemble of microstates corresponding to a given macrostate.

This is not the only purpose of this new approach. Indeed Statistical Mechanics, with respect to thermodynamics, makes more predictions describing the deviations from the average system's physical behaviour.

Statistical mechanics was initially created as an equilibrium theory, suitable for explaining the emergence of an equilibrium state for a macrostate, starting from a probabilistic study on microstates. Such equilibrium states are stationary states, stable in case of small perturbations.

Since the 19th century until now, a huge and powerful equilibrium sta-

tistical mechanics theory has been developed. In particular, detailed phase space diagrams, scaling laws and universality of the systems allow us to describe almost any equilibrium system. The concept of universality is worthy of attention: equilibrium systems have indeed been proved to be largely independent on the model's details. Very different systems, sharing certain fundamental symmetries, have the same behaviour in particular *critical* conditions.

What happens if the system is not at equilibrium? Thermodynamically there is a theory that was developed by Onsager for systems close to equilibrium [18]. Furthermore, under some assumptions, a non-equilibrium system can be described as sum of weakly interacting equilibrium subsystems.

The study of nonequilibrium systems is conceptually way more difficult. Indeed, in addition to the study of stationary fluctuations, in this case we are also interested in the dynamics of the system which evolves in time. Formally, for an equilibrium system, the distribution of the system's observables can be described by random variables. Instead, out of equilibrium, because of the instability of the system over time, stochastic processes are needed.

A stochastic process is therefore a very important tool in non-equilibrium statistical processes and an important part of the present day research is committed to analysing stochastic processes that are physically relevant.

As we said before, statistical mechanics has been proven to be successful at describing physical systems at thermodynamic equilibrium. But since most natural phenomena occur in nonequilibrium conditions, the present challenge is to find physical approaches for such conditions. Nonequilibrium statistical mechanics indeed does not exist as a systematic physical theory.

The present day work is mainly focused on the study of specific models. The analysis and collection of nonequilibrium models is a starting point in order to reach the ultimate goal: the construction of a full nonequilibrium statistical mechanics theory.

The application field of nonequilibrium physics is huge. Ecological and biological systems, optimal transportation network, complex networks dynamics and environmental science are based on nonequilibrium.

In particular, understanding the origin, maintenance and loss of biodiversity in ecological systems is a goal of the highest scientific priority given the rapidity of global biodiversity loss. Ecological communities exhibit pervasive patterns and relationships between size, abundance and the availability of resources [13]. And nonequilibrium statistical mechanics is the natural candidate to develop a unified framework for understanding the distribution of organism sizes, their energy use, and spatial distribution.

Bacterial suspensions, flocks of birds and swarms of insects, for instance, are self-propelled and interacting systems that, under proper conditions, display collective motion, aggregation and patterning. If one neglects the details of these systems, each individual can be described as a particle that

burns internal energy to move in the environment. Hence these systems are intrinsically out of equilibrium.

Their statistical properties such as the aggregation phenomena and dynamical patterning that occurs as a result of spatial confinement and the mechanisms of communication between individuals have to be studied by considering the non-equilibrium properties of such systems.

Pattern formation in particular is one of the most surprising aspects of nonequilibrium systems [17], [4], [3]. The complex patterns that appear everywhere in nature have been cause for wonder and fascination throughout human history [16]. People have always admired the elegance of the even simplest living systems.

The growing understanding of the physics of pattern formation has led to possibly speculate about a more general science of complexity, and to pose deep questions about our ability to predict and control natural phenomena.

The beauty of nature that surrounds us is based on equally beautiful mathematical equations that perfectly explain the emergence of so many surprising behaviours in all living systems. And this is what this thesis tries, at least partially, to deal with.

The purpose of this thesis is to analyse a particular nonequilibrium system characterized by the emergence of a crystal pattern formation. The work is based on a series of articles written by Christian Maes and Karel Netočný ([11],[12]) and tries to further develop the arguments of such papers. In particular the thesis is organized as follows. In the first chapter some theoretical notions about diffusion of particles subject to forces are introduced. In chapter 2 we explain the model of the system and start to analyse the features of the dynamics by computing the driving induced forces on the probes. In chapters 3, 4 and 5 the relaxation to a crystal pattern emerges and we study the stability of such a configuration. In the last chapter, finally, we analyse the thermodynamic limit of the system.

I would like to thank Professor Christian Maes for his constant guidance and endless supply of fascinating ideas for my research. I am most grateful for his constant and supportive supervision.

Thanks to his contagious curiosity and invaluable advice the work on my thesis turned into a really challenging opportunity.

I am also thankful to the KU Leuven Theoretical Physics department for its warm hospitality and support.

Finally, I would like to thank Professor Marco Baiesi for the suggestions and discussions that helped me during these months abroad.

Chapter 1

Theoretical background

In this first chapter we want to introduce the theoretical framework in which this thesis work is inserted.

In particular the features of a diffusing particle subject to external forces will be analysed.

1.1 Fokker-Planck equation

Let us start by considering a particle moving on a uniform one-dimensional lattice ($x_i = i \cdot l, t_n = n \cdot \epsilon$) and satisfying the Markovian property, meaning that the probability $W_i(t_{n+1})$ of being at the position labelled by i at the time-step t_{n+1} depends only on the state at t_n , that is on the probabilities $W_j(t_n) \forall j$ and on the transition probabilities $W_{ij}(t_n)$ from j to i :

$$W_i(t_{n+1}) = \sum_{j=-\infty}^{+\infty} W_{ij}(t_n) W_j(t_n) \quad (1.1)$$

Allowing jumps of any size in \mathbb{R} , (1.1) becomes:

$$W(x, t_{n+1}) = \int_{-\infty}^{+\infty} dz W(x, t_{n+1} | x - z, t_n) W(x - z, t_n) \quad (1.2)$$

The integrand is the probability of the particle being in $[x - z, x - z + dx]$ at time t_n and making a jump of size z to reach $[x, x + dx]$ at time t_{n+1} . By summing over all possible jump sizes we compute the total probability of the particle being near the arrival position. If we require jumps to be independent of each other then the jump probabilities $W(x, t_{n+1} | x - z, t_n)$ depend only on the jump size z . Assuming an isolate system, as the particle

cannot escape, probability is conserved:

$$\begin{aligned}
\int_{\mathbb{R}} dx W(x, t_{n+1}) &\stackrel{!}{=} \int_{\mathbb{R}} dy W(y, t_n) \\
&= \int_{\mathbb{R}} dz \int_{\mathbb{R}} dx W(x, t_{n+1} | x - z, t_n) W(x - z, t_n) = \\
&= \int_{\mathbb{R}} dz \int_{\mathbb{R}} dy W(y + z, t_{n+1} | y, t_n) W(y, t_n) = \\
&\stackrel{(a)}{=} \left(\int_{\mathbb{R}} dz W(\bar{y} + z, t_{n+1} | \bar{y}, t_n) \right) \left(\int_{\mathbb{R}} dy W(y, t_n) \right) \quad \forall \bar{y} \in \mathbb{R}
\end{aligned}$$

where in (a) we used the independent increments property (\bar{y} is an arbitrary constant). Comparing the first and last lines leads to:

$$\int_{\mathbb{R}} dz W(y + z, t_{n+1} | y, t_n) = 1 \tag{1.3}$$

Intuitively, if the particle cannot disappear, it must make a jump. For simplicity we denote

$$W(y + z, t_{n+1} | y, t_n) \equiv W(+z | y, t_n) \tag{1.4}$$

Starting from (1.2) and taking the continuum limit in time we can find a general diffusion equation. We start by constructing the difference quotient:

$$\begin{aligned}
W(x, t_{n+1}) - W(x, t_n) &= \int_{\mathbb{R}} dz W(+z | x - z, t_n) W(x - z, t_n) - W(x, t_n) = \\
&= \int_{\mathbb{R}} dz W(+z | x - z, t_n) W(x - z, t_n) - \int_{\mathbb{R}} dz W(+z | x, t_n) W(x, t_n) = \\
&= \int_{\mathbb{R}} dz \underbrace{[W(+z | x - z, t_n) W(x - z, t_n)]}_{F_z(x-z)} - \underbrace{[W(+z | x, t_n) W(x, t_n)]}_{F_z(x)} = \\
&= \int_{\mathbb{R}} dz [F_z(x - z) - F_z(x)] = \\
&= \int_{\mathbb{R}} dz \left[F_z(x) - z \frac{\partial}{\partial x} F_z(x) + \frac{z^2}{2} \frac{\partial^2}{\partial x^2} F_z(x) + \dots - F_z(x) \right] = \\
&= - \int_{\mathbb{R}} dz z \frac{\partial}{\partial x} [F_z(x)] + \frac{1}{2} \int_{\mathbb{R}} dz z^2 \frac{\partial^2}{\partial x^2} [F_z(x)] + \dots = \\
&= - \frac{\partial}{\partial x} \left[\left(\int_{\mathbb{R}} dz z W(+z | x, t_n) \right) W(x, t_n) \right] + \\
&\quad + \frac{1}{2} \frac{\partial^2}{\partial x^2} \left[\left(\int_{\mathbb{R}} dz z W(+z | x, t_n) \right) W(x, t_n) \right] + \dots \tag{1.5}
\end{aligned}$$

where $F_z(x)$ is the probability of a jump of size z from the position x . So at the end:

$$W(x, t_{n+1}) - W(x, t_n) = \sum_{k=1}^{+\infty} \frac{(-1)^k}{k!} \frac{\partial^k}{\partial x^k} (\mu_k(x, t_n) W(x, t_n)) \quad (1.6)$$

where we defined the k -th moment of the jump pdf as

$$\mu_k(x, t) = \int_{\mathbb{R}} dz z^k W(+z|x, t) \quad (1.7)$$

And consequently

$$\frac{W(x, t_{n+1}) - W(x, t_n)}{t_{n+1} - t_n} = \frac{\partial}{\partial x} \left\{ \sum_{k=1}^{\infty} \frac{(-1)^k}{k!} \frac{\partial^{k-1}}{\partial x^{k-1}} \frac{\mu_k(x, t_n) W(x, t_n)}{t_{n+1} - t_n} \right\} \quad (1.8)$$

Letting $t_{n+1} - t_n = \epsilon$, in the limit $\epsilon \rightarrow 0$ the left side will be $\dot{W}(x, t)$.

Assuming a gaussian pdf for the displacements:

$$z \sim \frac{1}{\sqrt{4\pi D\epsilon}} \exp\left(-\frac{(\Delta x)^2}{4D\epsilon}\right)$$

the first two moments become:

$$\mu_1 = 0 \quad \mu_2 = 2D\epsilon \quad (1.9)$$

And the variance

$$\text{Var}(z) = \mu_2 - \mu_1^2 = 2D\epsilon \quad (1.10)$$

However, for a particle subject to a force we would expect to have a preferred jump direction, leading to a constant velocity motion in the direction of the force. So we require a different μ_1 :

$$\mu_1 = \int_{\mathbb{R}} z W(+z|x, t) \propto \epsilon f(x) \quad (1.11)$$

We want to fix the variance to be proportional to ϵ , as it is expected in a diffusion process.

An appropriate choice for such a distribution is given by:

$$W(+z|x, t) = \frac{1}{\sqrt{\epsilon \hat{D}(x, t)}} F\left(\frac{z - \epsilon f(x, t)}{\sqrt{\epsilon \hat{D}(x, t)}}\right) \quad (1.12)$$

with $F, \hat{D} : \mathbb{R} \rightarrow \mathbb{R}$ functions, satisfying certain conditions, and with a physical meaning that we will see. First of all, we check the normalization:

$$1 \stackrel{!}{=} \int_{\mathbb{R}} dz W(+z|x, t) = \frac{1}{\sqrt{\epsilon \hat{D}(x, t)}} \int_{\mathbb{R}} dz F\left(\frac{z - \epsilon f(x, t)}{\sqrt{\epsilon \hat{D}(x, t)}}\right) = \int_{\mathbb{R}} dy F(y) \quad (1.13)$$

where in (a) we changed variables:

$$y = \frac{z - \epsilon f(x, t)}{\sqrt{\epsilon \hat{D}(x, t)}} \quad dz = \sqrt{\epsilon \hat{D}(x, t)} dy \quad (1.14)$$

Then we compute the first moment:

$$\begin{aligned} \langle z \rangle &= \mu_1(x, t) = \int_{\mathbb{R}} dz z F \left(\frac{z - \epsilon f(x, t)}{\sqrt{\epsilon \hat{D}(x, t)}} \right) \frac{1}{\sqrt{\epsilon \hat{D}(x, t)}} = \\ &= \int_{\mathbb{R}} dy (\epsilon f(x, t) + y \sqrt{\epsilon \hat{D}(x, t)}) F(y) = \\ &= \epsilon f(x, t) \underbrace{\int_{\mathbb{R}} F(y) dy}_{=1} + \sqrt{\epsilon \hat{D}(x, t)} \int_{\mathbb{R}} y F(y) dy \stackrel{!}{=} \epsilon f(x, t) \end{aligned}$$

So, in order to have the right normalization and the desired $\langle z \rangle$ we need:

$$\begin{cases} \int_{\mathbb{R}} dy F(y) = 1 \\ \int_{\mathbb{R}} dy y F(y) = 0 \end{cases}$$

For the second moment:

$$\begin{aligned} \mu_2(x, t) &= \frac{1}{\sqrt{\epsilon \hat{D}(x, t)}} \int_{\mathbb{R}} dz z^2 F \left(\frac{z - \epsilon f(x, t)}{\sqrt{\epsilon \hat{D}(x, t)}} \right) = \\ &= \int_{\mathbb{R}} dy (\epsilon f(x, t) + y \sqrt{\epsilon \hat{D}(x, t)})^2 F(y) = \\ &= \int_{\mathbb{R}} dy F(y) \left[\epsilon^2 f^2 + y^2 \hat{D} \epsilon + 2\epsilon \sqrt{\epsilon \hat{D}} f y \right] = \\ &= \epsilon^2 f^2 + \hat{D} \epsilon \int_{\mathbb{R}} dy y^2 F(y) = \epsilon^2 f^2 + \hat{D} \epsilon \langle y^2 \rangle_{F(y)} \quad (1.15) \end{aligned}$$

And so the variance becomes:

$$\text{Var}(z) = \mu_2 - \mu_1^2 = \epsilon \hat{D} \langle y^2 \rangle_{F(y)} \propto \epsilon \quad (1.16)$$

which is proportional to ϵ as desired. For notational simplicity, we introduce a new function $D : \mathbb{R} \rightarrow \mathbb{R}$ such that:

$$\text{Var}(z) = \epsilon \hat{D} \langle y^2 \rangle_{F(y)} \equiv 2D(x, t) \epsilon \Rightarrow \mu_2(x, t) = \epsilon^2 f^2 + 2D(x, t) \quad (1.17)$$

We note that higher order moments are all of order $O(\epsilon^{3/2})$. For example,

the third moment is:

$$\begin{aligned}
\mu_3(x, t) &= \frac{1}{\sqrt{\epsilon \hat{D}(x, t)}} dz \int_{\mathbb{R}} z^3 F \left(\frac{z - \epsilon f(x, t)}{\sqrt{\epsilon \hat{D}(x, t)}} \right) = \\
&= \int_{\mathbb{R}} dy (\epsilon f(x, t) + y \sqrt{\epsilon \hat{D}(x, t)})^3 F(y) = \\
&= \int_{\mathbb{R}} dy \left(\epsilon^3 f^3 + y^3 (\epsilon \hat{D})^{3/2} + 3\epsilon^2 f^2 y \sqrt{\epsilon \hat{D}} + 3\epsilon^2 f \hat{D} y^2 \right) F(y) = \\
&= \epsilon^3 f^3 + (\epsilon \hat{D})^{3/2} + 3\epsilon^2 f \hat{D} \langle y^2 \rangle_{F(y)} = O(\epsilon^{3/2})
\end{aligned}$$

Substituting (1.12) in (1.8), we get

$$\begin{aligned}
\frac{W(x, t_{n+1}) - W(x, t_n)}{\epsilon} &= -\frac{\partial}{\partial x} \left[W(x, t_n) \underbrace{\frac{\mu_1(x, t_n)}{\epsilon}}_{f(x, t)} \right] + \frac{1}{2} \frac{\partial^2}{\partial x^2} \left[W(x, t_n) \underbrace{\frac{\mu_2(x, t_n)}{\epsilon}}_{\epsilon f^2 + 2D(x, t)} \right] \\
&\quad + \underbrace{\frac{1}{3!} \frac{\partial^3}{\partial x^3} \left[W(x, t_n) \frac{\mu_3(x, t_n)}{\epsilon} \right]}_{O(\epsilon^{1/2})} + \dots \quad (1.18)
\end{aligned}$$

Taking the limit $\epsilon \rightarrow 0$ we obtain the **Fokker-Planck equation**, that is

$$\frac{\partial W(x, t)}{\partial t} = -\frac{\partial}{\partial x} \left[f(x, t) W(x, t) - \frac{\partial}{\partial x} (D(x, t) W(x, t)) \right] \quad (1.19)$$

and describes the diffusion process in the presence of a force $f(x, t)$ and a diffusion parameter $D(x, t)$.

Note that, in absence of forces and with a constant diffusion coefficient, from (1.19) we get the diffusion equation:

$$\frac{\partial}{\partial t} W(x, t) = D \frac{\partial^2}{\partial x^2} W(x, t) \quad (1.20)$$

Fokker-Planck equation (1.19) can be seen also as a Master equation with current $j(x, t)$:

$$\frac{\partial}{\partial t} W_t(x) + \frac{\partial}{\partial x} j(x, t) = 0, \quad j(x, t) = f(x, t) W(x, t) - \frac{\partial}{\partial x} (D(x, t) W(x, t)) \quad (1.21)$$

and in particular stationarity implies that

$$\frac{\partial}{\partial x} j(x, t) = 0. \quad (1.22)$$

1.2 Langevin equation

The Fokker-Planck equation involves probability distributions, meaning that it describes the behaviour of ensembles of trajectories at once. However, we can find an equivalent description by focusing on a single path. We start with a Wiener process, that is a stochastic process with independent and gaussian increments and continuous paths. Considering a time discretization $\{t_i\}$, the evolution of a single trajectory is described by:

$$x(t_{i+1}) = x(t_i) + \Delta x(t_i) \quad (1.23)$$

where each increment $\Delta x(t_i)$ is sampled from a gaussian pdf:

$$\Delta x_i(t_i) \sim \frac{1}{\sqrt{4\pi D \Delta t_i}} \exp\left(-\frac{(\Delta x)^2}{4D \Delta t_i}\right) \quad (1.24)$$

To simplify notation, we change variables, so that:

$$\frac{\Delta B^2}{2} = \frac{\Delta x^2}{4D} \Rightarrow \Delta B = \frac{\Delta x}{\sqrt{2D}} \quad (1.25)$$

If $x \sim p(x)$, and $y = y(x) \sim g(y)$, then by the rule for a change of random variables we have:

$$g(y) = p(x(y)) \frac{dx(y)}{dy} \quad (1.26)$$

In this case:

$$\Delta B \sim \frac{1}{\sqrt{4\pi D \Delta t_i}} \exp\left(-\frac{(\Delta B)^2}{2\Delta t_i}\right) \underbrace{\frac{d\Delta x}{d\Delta B}}_{\sqrt{2D}} = \frac{1}{\sqrt{2\pi \Delta t_i}} \exp\left(-\frac{(\Delta B)^2}{2\Delta t_i}\right) \quad (1.27)$$

Note that now $\langle \Delta B^2(t_i) \rangle = \Delta t_i$. So, in a sense, it is the "standard" Brownian path, and any specific Brownian motion can be obtained by rescaling it.

Substituting in (1.23) and rearranging we get:

$$x(t_{i+1}) - x(t_i) = \sqrt{2D} \Delta B(t_i) \quad (1.28)$$

Now we would like to have a time derivative in the left side, in order to obtain a stochastic differential equation for paths. In order to do this, we first extract a Δt_i factor from $\Delta B(t_i)$ by performing another change of variables:

$$\Delta B(t_i) \equiv \Delta t_i \xi(t_i) \quad (1.29)$$

so that $\Delta x_i = \sqrt{2D} \Delta t_i \xi_i$, and all the randomness is now contained in the random variable ξ , which is distributed according to:

$$\xi(t_i) \sim \frac{1}{\sqrt{2\pi\Delta t_i}} \exp\left(-\frac{\Delta t_i^2 \xi_i^2}{2\Delta t_i}\right) \underbrace{\frac{d\Delta B_i}{d\xi(t_i)}}_{\Delta t_i} = \sqrt{\frac{\Delta t_i}{2\pi}} \exp\left(-\frac{\Delta t_i}{2} \xi_i^2\right) \quad \xi_i \equiv \xi(t_i)$$

Substituting back in (1.28) and dividing by Δt_i leads to:

$$\frac{x(t_{i+1}) - x(t_i)}{\Delta t_i} = \sqrt{2D} \xi(t_i) \quad (1.30)$$

And by taking the continuum limit $\Delta t_i \rightarrow 0$ we get the Langevin equation for a Brownian particle:

$$\dot{x}(t) = \sqrt{2D} \xi(t) \quad (1.31)$$

We can see $\xi(t)$ as a highly irregular, quickly varying function, which, in a certain sense, expresses the result of Brownian collisions at a certain instant. In particular, the following holds:

$$\langle \xi(t) \rangle = 0 \quad \langle \xi(t) \xi(t') \rangle = \delta(t - t') \quad (1.32)$$

meaning that the values of $\xi(t)$ at different instants are completely independent. Brownian paths are not differentiable, so $\dot{x}(t)$ does not exist and (1.31) is just a formal equation, with a definite meaning only in a given discretization. In particular, as $\xi(t)$ is a random variable, eq. (1.31) is an example of a stochastic differential equation.

We can rewrite (1.31) in a more rigorous form by "multiplying by dt ", i.e. performing the change of variables (1.29), which, in the continuum limit, is $dB = \xi dt$, leading to:

$$dx(t) = \sqrt{2D} dB \quad dB \sim \frac{1}{\sqrt{2\pi dt}} \exp\left(-\frac{dB^2}{2 dt}\right) \quad (1.33)$$

Equations (1.31) and (1.33) can be generalized to the presence of external forces. This just results in adding a constant velocity motion to the particle, leading to the full **Langevin equation**:

$$\begin{aligned} \dot{x}(t) &= f(x, t) + \sqrt{2D(x, t)} \xi(t) \\ dx(t) &= f(x, t)dt + \sqrt{2D(x, t)} dB \quad dB \sim \frac{1}{\sqrt{2\pi dt}} \exp\left(-\frac{dB^2}{2 dt}\right) \end{aligned} \quad (1.34)$$

Consider a particle of mass m immersed in a fluid, with a radius a that is much larger than the surrounding molecules. The forces acting on it will be that of viscous friction $-\gamma\dot{\mathbf{r}}$, eventual external forces \mathbf{F}_{ext} and a

rapidly varying and random term $\mathbf{F}_{\text{noise}}$, encompassing the effect of the large number of collisions with the smaller fluid particles:

$$m\ddot{\mathbf{r}}(t) = -\gamma\dot{\mathbf{r}} + \mathbf{F}_{\text{ext}} + \mathbf{F}_{\text{noise}}(t) \quad (1.35)$$

Dividing both sides by γ :

$$\frac{m}{\gamma}\ddot{\mathbf{r}}(t) = -\dot{\mathbf{r}} + \frac{\mathbf{F}_{\text{ext}}(\mathbf{r}, t)}{\gamma} + \frac{\mathbf{F}_{\text{noise}}(t)}{\gamma} \quad (1.36)$$

If $\frac{m}{\gamma}$ is much smaller than the timescale we are interested in, we can neglect the acceleration term, reaching the overdamped limit for which (1.36) becomes:

$$\dot{\mathbf{r}} = \frac{\mathbf{F}_{\text{ext}}}{\gamma} + \frac{\mathbf{F}_{\text{noise}}}{\gamma} \quad (1.37)$$

In particular for a particle moving in one dimension:

$$\dot{x}(t) = \frac{F_{\text{ext}}}{\gamma} + \frac{F_{\text{noise}}}{\gamma} \quad (1.38)$$

Comparing (1.38) with (1.34) gives the physical meaning of $f(x, t)$ and $D(x, t)$.

Chapter 2

The model

The analysed model consists of a ring in which passive probes are suspended in a driven colloidal fluid. The red arrows in figure 2.1 indicate the fact that the colloids are driven by a rotational force ε . The thermal environment is then represented by the many smaller (blue) particles.

For a system of N probes, their coordinates are defined by x_α where α goes from 1 to N . The colloids are instead modeled via independent particles, have generic coordinate η and are subject to thermal noise.

In particular, for the colloids, an average density ρ^0 can be defined such that the number of colloids is $\rho^0 L$, where L is the length of the ring.

The only interaction considered in such a model is a local interaction between probes and colloids which interact through a local potential $u(x_\alpha - \eta)$ such that $u(z) = u(-z)$ and $u(z) = 0$ for $|z| > \delta$. Therefore δ is the range of the interaction.

The starting point for such an analysis is the study of the colloids' dynamics. The colloidal fluid is driven and subject to thermal noise. Thus it can be described by the overdamped Langevin equation

$$\zeta \frac{d\eta_t}{dt} = \varepsilon - \frac{\partial U(x, \eta_t)}{\partial \eta} + \left(\frac{2\zeta}{\beta}\right)^{1/2} \xi_t \quad (2.1)$$

where $U(x, \eta) = \sum_\alpha u(x_\alpha - \eta)$, $\varepsilon \geq 0$ is the constant driving force and ζ is the fixed friction parameter.

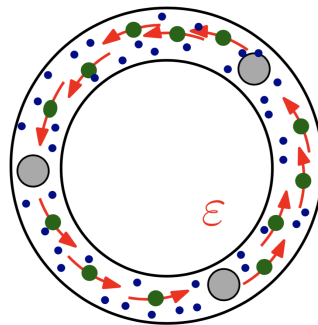


Figure 2.1: *Passive probes suspended in a driven colloidal fluid. The big grey particles are the probes, the arrowed green particles are the driven colloids and the small blue particles represent the thermal environment.*

Due to the local interaction $u(x_\alpha - \eta)$ the mean force on the α -th probe from the driven fluid is

$$f_\alpha(x) = - \int_0^L u'(x_\alpha - \eta) \rho_x(\eta) d\eta \quad (2.2)$$

where the classical definition of the force averaged on the colloid density $\rho_x(\eta)$ has been used.

In particular

$$u'(x_\alpha - \eta) = \frac{\partial u(x_\alpha - \eta)}{\partial x_\alpha} = \frac{\partial U(x, \eta_t)}{\partial x_\alpha} \quad (2.3)$$

In order to compute eq. (2.2) the stationary colloidal density is needed and that will be done in section 2.1.

From the Langevin equation (2.1) easily follows the Smoluchowski equation

$$\zeta \frac{\partial \rho_t(\eta)}{\partial t} = - \frac{\partial}{\partial \eta} \left[\left(\varepsilon - \frac{\partial U}{\partial \eta} \right) \rho_t(\eta) \right] + \frac{\partial^2}{\partial \eta^2} \left(\frac{\rho_t(\eta)}{\beta} \right) \quad (2.4)$$

that describes the colloidal density and from which the current $j(\eta)$ of the colloid flow is defined such that

$$\frac{\partial}{\partial t} \rho_t(\eta) + \frac{\partial}{\partial \eta} j(\eta) = 0 \quad (2.5)$$

The (stationary) Smoluchowski equation (2.4) can thus be rewritten as

$$\zeta j_x = \rho_x(\eta) \left[\varepsilon - \frac{\partial U}{\partial \eta} \right] - \frac{\rho'_x(\eta)}{\beta} \quad (2.6)$$

For the forces the following transmission rule can then be derived

$$\begin{aligned} \sum_\alpha f_\alpha(x) &= - \sum_\alpha \oint \frac{\partial U(x, \eta)}{\partial x_\alpha} \rho_x(\eta) d\eta = \oint \frac{\partial U(x, \eta)}{\partial \eta} \rho_x(\eta) d\eta = \\ &= \oint (\rho_x(\eta) \varepsilon - \zeta j_x) d\eta = \varepsilon \rho^0 L - \zeta j_x L = (\varepsilon \rho^0 - \zeta j_x) L \end{aligned} \quad (2.7)$$

where we used equation (2.6) and the fact that $\oint d\eta \rho'_x(\eta) = 0$ as obviously the density has an L-periodicity where L is the length of the ring.

2.1 Stationary density of the driven colloidal fluid

The explicit solution of the Smoluchowski equation has the form of a marginal density

$$\rho_x(\eta) = \int_0^L \mu_x(\eta, \eta') d\eta' \quad (2.8)$$

where

$$\mu_x(\eta, \eta') = \frac{\rho^0 L}{\Omega(x)} e^{-\beta W_x(\eta, \eta')} \quad (2.9)$$

$$\Omega(x) = \int_0^L \int_0^L e^{-\beta W_x(\eta, \eta')} d\eta d\eta' \quad (2.10)$$

$$W_x(\eta, \eta') = U(x, \eta) - U(x, \eta') + \begin{cases} \varepsilon (\eta' - \eta)^o & \text{for } \varepsilon \geq 0 \\ -\varepsilon (\eta - \eta')^o & \text{for } \varepsilon \leq 0 \end{cases} \quad (2.11)$$

where $(\eta' - \eta)^o$ stands for $\eta' - \eta \bmod L$ and so, explicitly,

$$(\eta' - \eta)^o = \begin{cases} \eta' - \eta & \text{if } \eta' > \eta \\ L - (\eta - \eta') & \text{if } \eta' < \eta \end{cases} \quad (2.12)$$

The integral can therefore be divided in two terms.

$$\rho_x(\eta) = \frac{\rho^0 L}{\Omega(x)} e^{-\beta U(x, \eta)} \left[\int_0^\eta e^{\beta U(x, \eta') - \beta \varepsilon [L - (\eta - \eta')]} d\eta' + \int_\eta^L e^{\beta U(x, \eta') - \beta \varepsilon (\eta' - \eta)} d\eta' \right] \quad (2.13)$$

Here is the proof that (2.8) is the correct stationary colloidal density.

From the Smoluchowski equation (2.4), the stationary density should satisfy

$$0 = \frac{\partial}{\partial \eta} \left[\left(\varepsilon - \frac{\partial U}{\partial \eta} \right) \rho_x(\eta) - \frac{\partial}{\partial \eta} \left(\frac{\rho_x(\eta)}{\beta} \right) \right] \quad (2.14)$$

Using (2.13) the derivative inside the square brackets can be rewritten as

$$\frac{\partial}{\partial \eta} \left(\frac{\rho_x(\eta)}{\beta} \right) = \left[\rho_x(\eta) \left(-\frac{\partial U}{\partial \eta} + \varepsilon \right) + \frac{\rho^0 L}{\beta \Omega(x)} e^{-\beta U(x, \eta) + \beta \varepsilon \eta} \left(e^{\beta U(x, \eta) - \beta \varepsilon (L + \eta)} - e^{\beta U(x, \eta) - \beta \varepsilon \eta} \right) \right] \quad (2.15)$$

from which

$$\begin{aligned} \left(\varepsilon - \frac{\partial U}{\partial \eta} \right) \rho_x(\eta) - \frac{\partial}{\partial \eta} \left(\frac{\rho_x(\eta)}{\beta} \right) &= -\frac{\rho^0 L}{\beta \Omega(x)} e^{-\beta U(x, \eta) + \beta \varepsilon \eta} e^{\beta U(x, \eta) - \beta \varepsilon \eta} (e^{-\beta \varepsilon L} - 1) \\ &= -\frac{\rho^0 L}{\beta \Omega(x)} (e^{-\beta \varepsilon L} - 1) \end{aligned} \quad (2.16)$$

This means that the expression inside the square brackets in (2.14) does not depend on η and therefore equation 2.14 is satisfied.

It is also possible to find some useful identities for the current.

Dividing equation (2.6) by ρ_x and integrating it in η around the ring the following expression is obtained:

$$\zeta j_x \oint \frac{d\eta}{\rho_x(\eta)} = \varepsilon L + \oint \left[-\frac{\partial U}{\partial \eta}(x, \eta) - \frac{1}{\beta} \frac{\rho'_x(\eta)}{\rho_x(\eta)} \right] d\eta \quad (2.17)$$

and since the integral on the right vanishes because of periodicity

$$j_x = \frac{\varepsilon L}{\zeta \oint \frac{d\eta}{\rho_x(\eta)}} \quad (2.18)$$

from which

$$\int_0^L \frac{d\eta}{\rho_x(\eta)} = \frac{\varepsilon L}{j_x \zeta}. \quad (2.19)$$

A consequence of the Cauchy-Schwarz inequality, Titu's lemma, can now be considered [14]. The lemma states that, for positive real u_i and v_i

$$\frac{(\sum_{i=1}^n u_i)^2}{\sum_{i=1}^n v_i} \leq \sum_{i=1}^n \frac{u_i^2}{v_i} \quad (2.20)$$

This can clearly be rewritten as

$$\frac{(\frac{L}{n} \sum_{i=1}^n u_i) (\frac{L}{n} \sum_{i=1}^n u_i)}{\frac{L}{n} \sum_{i=1}^n v_i} \leq \frac{L}{n} \sum_{i=1}^n \frac{u_i^2}{v_i} \quad (2.21)$$

Imagine now to divide the length L of the ring in n segments. For each of these segments (labeled with index i) consider $u_i = 1$ and $v_i = \rho_{x_i}(\eta)$ where $\rho_{x_i}(\eta)$ is the colloidal density in the mid point of segment i .

Substituting this in 2.21:

$$\frac{(\frac{L}{n} \sum_{i=1}^n 1) (\frac{L}{n} \sum_{i=1}^n 1)}{\frac{L}{n} \sum_{i=1}^n \rho_{x_i}(\eta)} \leq \frac{L}{n} \sum_{i=1}^n \frac{1}{\rho_{x_i}(\eta)} \quad (2.22)$$

In the limit for $n \rightarrow \infty$

$$\frac{\left(\int_0^L d\eta\right)^2}{\int_0^L d\eta \rho_x(\eta)} \leq \int_0^L d\eta \frac{1}{\rho_x(\eta)} \quad (2.23)$$

And therefore from (2.19)

$$\frac{\varepsilon L}{j_x \zeta} = \int_0^L \frac{d\eta}{\rho_x(\eta)} \geq \frac{L^2}{\int_0^L d\eta \rho_x(\eta)} = \frac{L^2}{\rho^0 L} \quad (2.24)$$

from which we get for the current the bound:

$$\frac{\zeta j_x}{\varepsilon \rho^0} \leq 1 \quad (2.25)$$

It is possible also to express the stationary current in function of the normalization factor $\Omega(x)$. Indeed from equations (2.16) and (2.6) it is straightforward to get

$$j_x = \frac{\rho^0 L (1 - e^{-\beta \varepsilon L})}{\zeta \beta \Omega(x)} = \frac{\rho^0 \varepsilon}{\zeta Z(x)} \quad (2.26)$$

where in the last equality $Z(x)$ is the modified normalization function defined as

$$Z(x) = \frac{\beta \varepsilon}{L(1 - e^{-\beta \varepsilon L})} \Omega(x) \quad (2.27)$$

The factor inside the colloid density that contains the interaction is

$$e^{-\beta U(x,\eta)} = e^{-\beta \sum_{\alpha} u(x_{\alpha}-\eta)} = \prod_{\alpha} e^{-\beta u(x_{\alpha}-\eta)} \quad (2.28)$$

Introducing the Mayer expansion formula, it can be rewritten as

$$e^{-\beta U(x,\eta)} = \prod_{\alpha} [1 + \phi^{-}(x_{\alpha} - \eta)] \quad (2.29)$$

where $\phi^{-}(z) = e^{-\beta u(z)} - 1$.

The probes of the system are considered isolated, in the sense that $|x_{\alpha} - x_{\gamma}| \geq 2\delta$. This imposes an upper bound on the average density of probes $\frac{N}{L} \leq (2\delta)^{-1}$. Making this assumption, the colloidal particle of coordinate η cannot interact with two different probes and so

$$\prod_{\alpha} [1 + \phi^{-}(x_{\alpha} - \eta)] = 1 + \sum_{\alpha} \phi^{-}(x_{\alpha} - \eta) \quad (2.30)$$

The same reasoning can be used for $e^{\beta U(x,\eta)}$ using this time $\phi^{+}(z) = 1 - e^{\beta u(z)}$.

At the end

$$e^{-\beta U(x,\eta)} = 1 + \sum_{\alpha} \phi^{-}(x_{\alpha} - \eta) \quad e^{\beta U(x,\eta)} = 1 - \sum_{\alpha} \phi^{+}(x_{\alpha} - \eta) \quad (2.31)$$

It is possible now to use this in order to find a more explicit expression of the modified normalization function $Z(x)$.

First of all a new length scale emerges in the system. Indeed $l_d = (\beta\varepsilon)^{-1}$ is a length scale associated with the driving and it represents the typical distance on which the dissipation as measured via the entropy flux (see [9]) to the thermal bath becomes relevant.

In particular when $l_d \gg L$ the colloidal medium is (globally) close to equilibrium, but increasing the ring size L the colloidal fluid is driven further from equilibrium. In order to understand which is the most interesting regime to study, there are three different length scales to analyse (L , l_d and the interaction range δ) and the interplay between them is crucial.

Just by looking at equation (2.2) it is clear that the detailed structure of the forces depends on how the probes modify the stationary colloidal density $\rho_x(\eta)$. Under equilibrium conditions ($\varepsilon = 0$) this modification is just local (on the scale δ). Thus, for N isolated probes ($|x_{\alpha} - x_{\gamma}| \geq 2\delta$), the absence of the driving force makes the colloidal density almost homogenous, with N *bubbles* around the positions of the probes. Since these *bubbles* are symmetric and their supports do not intersect, under equilibrium all the forces on the probes vanish.

Instead, for driven colloids ($\varepsilon > 0$), the symmetry around the probes of the colloidal density *bubbles* breaks down.

As long as the entropy flux for a colloid moving along the ring is small ($l_d \gg L$) the medium is close to equilibrium and again there will be vanishing forces on the probes.

Also when the regime is too far from equilibrium, in the sense that the colloidal fluid is also locally strongly driven ($l_d \ll \delta$), again the non-equilibrium density *bubbles* become local (see [11]).

The globally strong but locally not so strong non-equilibrium regime ($2\delta < l_d \ll L$) will be then the most interesting one and the one analysed in this thesis.

In this nonequilibrium regime terms of order $O(e^{-\beta\varepsilon L})$ can be neglected and, considering (2.10), (2.11), (2.31), equation (2.27) can be written as

$$Z(x) = \frac{\beta\varepsilon}{L} \int_0^L d\eta \int_0^L d\eta' \left[1 - \sum_{\alpha} \phi^+(x_{\alpha} - \eta) \right] \left[1 + \sum_{\gamma} \phi^-(x_{\gamma} - \eta') \right] e^{-\beta\varepsilon(\eta' - \eta)^o} \quad (2.32)$$

The biggest problem of such an expression is the presence of the term $(\eta' - \eta)^o$ that needs to be treated carefully, reminding 2.12. The periodicity of the configuration allows to choose as extrema of the second integral η and $\eta + L$. In this way $(\eta' - \eta)^o = \eta' - \eta$.

From the multiplication of the square brackets of (2.32) four different terms (that will be integrated separately) are obtained:

$$\left[1 + \sum_{\gamma} \phi^-(x_{\gamma} - \eta') - \sum_{\alpha} \phi^+(x_{\alpha} - \eta) - \sum_{\alpha, \gamma} \phi^+(x_{\alpha} - \eta) \phi^-(x_{\gamma} - \eta') \right] \quad (2.33)$$

For the first one

$$\int_0^L d\eta \int_{\eta}^{\eta+L} d\eta' e^{-\beta\varepsilon(\eta' - \eta)} = \int_0^L d\eta e^{\beta\varepsilon\eta} \left[\frac{e^{-\beta\varepsilon\eta'}}{-\beta\varepsilon} \right]_{\eta}^{\eta+L} = \int_0^L d\eta \frac{e^{-\beta\varepsilon L} - 1}{-\beta\varepsilon} = \frac{L}{\beta\varepsilon} \quad (2.34)$$

where in the last equality $e^{-\beta\varepsilon L}$ was neglected, according to the globally strong driving regime.

The second and the third one are similar. In particular, reminding the interaction range δ and using that for the extrema of integration, the sum of the two terms becomes

$$\frac{N}{\beta\varepsilon} \int_{-\delta}^{\delta} dz [\phi^- - \phi^+](z) \quad (2.35)$$

The fourth term is then

$$\begin{aligned}
& \int_0^L d\eta \int_\eta^{\eta+L} d\eta' \sum_{\alpha,\gamma} \phi^+(\eta - x_\alpha) \phi^-(\eta' - x_\gamma) e^{-\beta\varepsilon(\eta' - \eta)^\circ} = \\
&= \int_0^L dz \int_z^{z+L} dz' \sum_{\alpha,\gamma} \phi^+(z) \phi^-(z' + x_\alpha - x_\gamma) e^{-\beta\varepsilon(z' - z)^\circ} = \\
&= \int_{-\delta}^\delta dz \int_z^{z+L} dz' \sum_{\alpha,\gamma} \phi^+(z) \phi^-(z' + x_\alpha - x_\gamma) e^{-\beta\varepsilon(z' - z)^\circ} \quad (2.36)
\end{aligned}$$

where $z' = \eta' - x_\alpha$ and $z = \eta - x_\alpha$.

At the end, considering also the factor $\frac{\beta\varepsilon}{L}$ in front of all the terms,

$$Z(x) = 1 + \frac{N}{L} \int_{-\delta}^\delta dz [\phi^- - \phi^+](z) - \frac{\beta\varepsilon}{L} \sum_{\alpha,\gamma} \int_{-\delta}^\delta dz \int_z^{z+L} dz' \phi^+(z) \phi^-(z' + x_\alpha - x_\gamma) e^{-\beta\varepsilon(z' - z)^\circ} \quad (2.37)$$

The contribution $\alpha = \gamma$ of the last term together with the second and third term depend on the probes only via their density and can be rewritten as $\frac{NA}{L}$, where

$$A = \int_{-\delta}^\delta \phi^- \phi^+(z) dz - \beta\varepsilon \int_{-\delta}^\delta \phi^-(z) e^{-\beta\varepsilon z} dz \int_{-\delta}^z \phi^+(z') e^{\beta\varepsilon z'} dz' \quad (2.38)$$

Now there are the contributions of the last term with $\alpha \neq \gamma$ left. Each term of the sum is of the form

$$\int_{-\delta}^\delta dz \int_z^{z+L} dz' \phi^+(z) \phi^-(z' + x_\alpha - x_\gamma) e^{-\beta\varepsilon(z' - z)^\circ} \quad (2.39)$$

where the fact that $(z' - z)^\circ = z' - z$ is assured by the extrema of the integral in dz' .

Set $y = z' - x_\alpha + x_\gamma$ the term can be rewritten as

$$\int_{-\delta}^\delta dz \phi^+(z) e^{\beta\varepsilon z} \int_{-\delta}^{-z + (x_\gamma - x_\alpha)^\circ} dy \phi^-(y) e^{+\beta\varepsilon y} e^{-\beta\varepsilon(x_\gamma - x_\alpha)^\circ} \quad (2.40)$$

The upper extreme of the integral and the last exponent come from the condition $z' > z$.

The fact that $\min(-z + (x_\gamma - x_\alpha)^\circ) = \delta$ and that $\phi^-(y) \neq 0$ only for $y \in [-\delta, \delta]$ allows to rewrite the terms as

$$\int_{-\delta}^\delta dz \phi^+(z) e^{\beta\varepsilon z} \int_{-\delta}^\delta dy \phi^-(y) e^{+\beta\varepsilon y} e^{-\beta\varepsilon(x_\gamma - x_\alpha)^\circ} \quad (2.41)$$

and considering also the prefactor

$$- \frac{\beta\varepsilon}{L} B \sum_{\alpha,\gamma \neq \alpha} e^{-\beta\varepsilon(x_\gamma - x_\alpha)^\circ} \quad (2.42)$$

where

$$B = B^+ B^- \quad B^{+(-)} = \int_{-\delta}^{\delta} \phi^{+(-)}(z) e^{\beta \varepsilon z} dz \quad (2.43)$$

At the end the modified normalization function can be written as

$$Z(x) = 1 + \frac{NA}{L} - \frac{\beta \varepsilon}{L} B \sum_{\alpha, \gamma \neq \alpha} e^{-\beta \varepsilon (x_\gamma - x_\alpha)^o} \quad (2.44)$$

Considering now the solution (2.8) of the colloidal density, it is possible to analyse the integral in η' . In particular the only factor of (2.9) that depends on η' is $e^{-\beta W_x(\eta, \eta')}$:

$$\begin{aligned} \int_0^L e^{-\beta W_x(\eta, \eta')} d\eta' &= e^{-\beta U(x, \eta)} \int_0^L e^{\beta U(x, \eta') - \beta \varepsilon (\eta' - \eta)^o} d\eta' & (2.45) \\ &= e^{-\beta U(x, \eta)} \int_\eta^{\eta+L} \left[1 - \sum_\alpha \phi^+(x_\alpha - \eta') \right] e^{-\beta \varepsilon (\eta' - \eta)} d\eta' \\ &= e^{-\beta U(x, \eta)} \int_\eta^{\eta+L} d\eta' \left[e^{-\beta \varepsilon (\eta' - \eta)} - \sum_\alpha \phi^+(x_\alpha - \eta') e^{-\beta \varepsilon (\eta' - \eta)} \right] \\ &= e^{-\beta U(x, \eta)} \left[\frac{1}{\beta \varepsilon} - \int_\eta^{\eta+L} \sum_\alpha \phi^+(x_\alpha - \eta') e^{-\beta \varepsilon (\eta' - \eta)} d\eta' \right] \end{aligned}$$

where terms $O(e^{-\beta \varepsilon L})$ were neglected. The last integral can be solved by rewriting it as

$$\int_\eta^{\eta+L} \sum_\alpha \phi^+(\eta' - x_\alpha) e^{-\beta \varepsilon (\eta' - \eta)} d\eta' \quad (2.46)$$

Defining now

$$z' = \eta' - x_\alpha \quad z = \eta - x_\alpha \quad \Phi(z) = \int_{-\delta}^z \phi^+(z') e^{\beta \varepsilon z'} dz' \quad (2.47)$$

the result is

$$\int_0^L e^{-\beta W_x(\eta, \eta')} d\eta' = e^{-\beta U(x, \eta)} \left[\frac{1}{\beta \varepsilon} - \sum_\alpha \Phi(x_\alpha - \eta) e^{-\beta \varepsilon (x_\alpha - \eta)} \right] \quad (2.48)$$

The stationary colloidal density in the strong driving regime (so neglecting terms of order $O(e^{-\beta \varepsilon L})$) is then

$$\begin{aligned} \rho_x(\eta) &= \frac{\rho^0 L}{\Omega(x)} \int_0^L e^{-\beta W_x(\eta, \eta')} \\ &= \frac{\rho^0 L \beta \varepsilon}{L(1 - e^{-\beta \varepsilon L}) Z(x)} e^{-\beta U(x, \eta)} \left[\frac{1}{\beta \varepsilon} - \sum_\alpha \Phi(x_\alpha - \eta) e^{-\beta \varepsilon (x_\alpha - \eta)} \right] \\ &= \frac{\rho^0 e^{-\beta U(x, \eta)}}{Z(x)} \left[1 - \beta \varepsilon \sum_\alpha \Phi(x_\alpha - \eta) e^{-\beta \varepsilon (x_\alpha - \eta)} \right] \end{aligned} \quad (2.49)$$

Anyway in the globally strong but locally weak driving regime, in which $\beta\varepsilon\delta \ll 1 \ll \beta\varepsilon L$, the ε -dependence of the form factors is negligible and they can be written as

$$A_\varepsilon = B_0^- - B_0^+ + O(\beta\varepsilon\delta) \quad B_\varepsilon^\pm = B_0^\pm + O((\beta\varepsilon\delta)^2) \quad B_0^\pm = \int_{-\delta}^{\delta} \phi^\pm(z) dz \quad (2.50)$$

2.2 Driving-induced forces

The force on the α -th probe can now be calculated using equation (2.2) and substituting in it the computed stationary colloidal density (2.49). In particular eq. (2.2) can be rewritten as

$$\begin{aligned} f_\alpha(x) &= \frac{1}{\beta} \oint \rho_x(\eta) e^{\beta U(x,\eta)} \frac{\partial}{\partial x_\alpha} \left[e^{-\beta U(x,\eta)} \right] \quad (2.51) \\ \text{from (2.31)} &= -\frac{1}{\beta} \oint \rho_x(\eta) e^{\beta U(x,\eta)} \frac{\partial}{\partial \eta} \left[\phi^-(x_\alpha - \eta) \right] d\eta \\ &= \frac{1}{\beta} \oint \phi^-(x_\alpha - \eta) \frac{\partial}{\partial \eta} \left[\rho_x(\eta) e^{\beta U(x,\eta)} \right] d\eta \\ &= \frac{1}{\beta} \oint \phi^-(x_\alpha - \eta) \frac{\partial}{\partial \eta} \left[\frac{\rho^0}{Z(x)} \left[1 - \beta\varepsilon \sum_\gamma \Phi(x_\gamma - \eta) e^{-\beta\varepsilon(x_\gamma - \eta)} \right] \right] d\eta \\ &= \oint \frac{-\varepsilon\rho^0}{Z(x)} \phi^- \sum_\gamma \left[\left(\frac{\partial}{\partial \eta} \Phi(x_\gamma - \eta) \right) e^{-\beta\varepsilon(x_\gamma - \eta)} + \Phi(x_\gamma - \eta) e^{-\beta\varepsilon(x_\gamma - \eta)} \beta\varepsilon \right] d\eta \end{aligned}$$

In particular the derivative of $\Phi(x_\gamma - \eta)$ is

$$\frac{\partial}{\partial \eta} \Phi(x_\gamma - \eta) = -\frac{\partial}{\partial z} \Phi(z) = -\frac{\partial}{\partial z} \int_{-\delta}^z \phi^+(z') e^{\beta\varepsilon z'} dz' = -\phi^+(z) e^{\beta\varepsilon z} \quad (2.52)$$

and thus

$$f_\alpha(x) = - \oint \frac{\varepsilon\rho^0}{Z(x)} \phi^-(x_\alpha - \eta) \sum_\gamma \left[-\phi^+(x_\gamma - \eta) + \Phi(x_\gamma - \eta) e^{-\beta\varepsilon(x_\gamma - \eta)} \beta\varepsilon \right] d\eta \quad (2.53)$$

Let us analyse the contribution of the term with $\gamma = \alpha$. This will be the α -independent drift component of the force and its expression is

$$f^{\text{drift}}(x) = \frac{\varepsilon\rho^0 A}{Z(x)} = \zeta j_x A \quad (2.54)$$

The contributions with $\gamma \neq \alpha$ provide instead the interaction component. Set $z = \eta - x_\alpha$ and $z' = \eta' - x_\alpha$ let us study the case $\gamma \neq \alpha$.

$$\begin{aligned}
f_{\alpha}^{\text{int}}(x) &= \frac{\varepsilon\rho^0}{Z(x)} \sum_{\gamma \neq \alpha} \left[\int_{-\delta}^{\delta} \phi^{-}(z)\phi^{+}(z+x_{\alpha}-x_{\gamma})dz + \right. \\
&\quad \left. -\beta\varepsilon \int_{-\delta}^{\delta} dz\phi^{-}(z) \int_{-\delta}^{x_{\gamma}-z-x_{\alpha}} \phi^{+}(z')e^{\beta\varepsilon z'}e^{-\beta\varepsilon(x_{\gamma}-x_{\alpha})}dz' \right] \quad (2.55)
\end{aligned}$$

The first term inside the sum is 0 because of the probes' isolation condition.

For the second term instead the same reasoning of equation (2.41) can be used and at the end

$$\begin{aligned}
f_{\alpha}^{\text{int}} &= -\frac{\beta\varepsilon^2\rho^0}{Z(x)} \sum_{\gamma \neq \alpha} \int_{-\delta}^{\delta} dz\phi^{-}(z)e^{\beta\varepsilon z} \int_{-\delta}^{\delta} \phi^{+}(z')e^{\beta\varepsilon z'}e^{-\beta\varepsilon(x_{\gamma}-x_{\alpha})}dz' \\
&= -\frac{\beta\varepsilon^2\rho^0}{Z(x)} B \sum_{\gamma \neq \alpha} e^{-\beta\varepsilon(x_{\gamma}-x_{\alpha})} \\
&= -\frac{\zeta j_x B}{l_d} \sum_{\gamma \neq \alpha} e^{-\frac{(x_{\gamma}-x_{\alpha})}{l_d}} \quad (2.56)
\end{aligned}$$

where in the last passage $l_d = (\beta\varepsilon)^{-1}$ and $j_x = \frac{\varepsilon\rho^0}{\zeta Z(x)}$ (2.26).

At the end the complete expression for the mean force on the α -th probe in the globally strong driving regime is

$$f_{\alpha}(x) = f^{\text{drift}}(x) + f_{\alpha}^{\text{int}}(x) = \zeta j_x A - \frac{\zeta j_x B}{l_d} \sum_{\gamma \neq \alpha} e^{-\frac{(x_{\gamma}-x_{\alpha})}{l_d}} \quad (2.57)$$

Considering the equidistant configuration, for which

$$x_{\alpha}^*(t) = v^*t + \frac{L}{N}\alpha, \quad (2.58)$$

equation (2.57) becomes

$$f_{\alpha}^{\text{int}}(x^*) = -\frac{\zeta j_x B}{l_d} \sum_{n=1}^{N-1} e^{-\frac{1}{l_d}\frac{L}{N}n} \quad (2.59)$$

where in the rightside of the equation is a finite geometric series that can be easily computed as

$$f_{\alpha}^{\text{int}}(x^*) = -\frac{\zeta j_x B}{l_d} \frac{e^{-\frac{L}{Nl_d}} - e^{-\frac{L}{l_d}}}{1 - e^{-\frac{L}{Nl_d}}} \quad (2.60)$$

In the globally strong driving approximation $e^{-\frac{L}{l_d}}$ can be neglected, such that

$$f_{\alpha}^{\text{int}}(x^*) = -\frac{\zeta j_x^* B}{l_d} \frac{1}{e^{\frac{L}{Nl_d}} - 1} \quad (2.61)$$

and the total force for the equidistant configuration is

$$f(x^*) = \zeta j_{x^*} \left(A - \frac{B}{l_d} \frac{1}{e^{\frac{L}{Nl_d}} - 1} \right) \quad (2.62)$$

Using geometric series also the modified normalization function (2.44) for the equidistant configuration can be written as

$$Z(x^*) = 1 + \frac{NA}{L} - \frac{\beta \varepsilon NB}{L} \frac{1}{e^{\frac{L}{Nl_d}} - 1} \quad (2.63)$$

From eq. (2.63), (2.26) and (2.7) a more explicit expression for the total force in the equidistant configuration can be computed. In particular

$$f(x^*) = \frac{\varepsilon \rho^0 L}{N} \left[1 - \frac{1}{Z(x^*)} \right] \quad (2.64)$$

Let us now go back to the more general case of equation (2.57). This force has been computed under some assumptions:

- Non-interacting colloids.
- Probes' isolation condition: $|x_\alpha - x_\gamma| \geq 2\delta \quad \forall \alpha \neq \gamma$, where δ is the probe-colloids interaction range.
- Globally strong driving regime: $l_d \equiv (\beta \varepsilon)^{-1} \ll L$.

In particular the interaction part is

$$f_\alpha^{\text{int}}(x) = -\frac{\zeta j_x B}{l_d} \sum_{\gamma \neq \alpha} e^{-\frac{(x_\gamma - x_\alpha)^0}{l_d}} \quad (2.65)$$

The force is of order ε^2 (due to the presence of j_x and l_d in the prefactor) and it is a **non-reactive** force, in the sense that it violates the action-reaction principle. In fact each probe is influenced by all the other probes which are ahead of it on the length scale l_d , but not vice versa.

This non reactive force can be both repulsive or attractive, depending on the sign of B .

We will have a repulsive force if $B > 0$ and so if B^+ and B^- have the same sign. In order to have that is sufficient for example to have a probe-colloid interaction $u(z)$ either completely positive or completely negative. Another sufficient condition is for example that the temperature is large enough such that B^+ and B^- become nearly equal (see equation (2.43)).

Chapter 3

Mechanical Stability of the crystal pattern

Now that the mean force on the probes has been computed, in this chapter the dynamics of the probes will be analysed. In particular the possibility of the stability of an equidistant, crystal pattern will be explored. The set of probes can be considered as an overdamped dynamical system where

$$\Gamma \dot{x}_\alpha = f_\alpha(x) \quad (3.1)$$

Their equidistant configuration

$$x_\alpha^*(t) = v^*t + \frac{L}{N}\alpha \quad (3.2)$$

forms a stationary cycle with steady rotation speed

$$v^* = \frac{f_\alpha(x^*)}{\Gamma} = \frac{\zeta j x^*}{\Gamma} \left(A - \frac{B}{l_d} \frac{1}{e^{\frac{L}{Nl_d}} - 1} \right) \quad (3.3)$$

The idea is to consider a small perturbation of the equidistant configuration, such that the probes' coordinates can be written as

$$x_\alpha = x_\alpha^* + y_\alpha \quad (3.4)$$

Due to the presence of a small perturbation the probes' dynamics can be linearized and the force can be rewritten to the first-order as

$$f_\alpha(x) = f_\alpha(x^* + y) = f_\alpha(x^*) + \sum_{\gamma} M_{\alpha\gamma} y_\gamma \quad (3.5)$$

where M is the stiffness matrix with $M_{\alpha\gamma} = \frac{\partial f_\alpha(x^*)}{\partial x_\gamma}$. Then, from the overdamped dynamics

$$f_\alpha(x) = \Gamma \dot{x}_\alpha = \Gamma \dot{x}_\alpha^* + \Gamma \dot{y}_\alpha. \quad (3.6)$$

From (3.5) and (3.6) comes directly that

$$\Gamma \dot{y}_\alpha = \sum_{\gamma} M_{\alpha\gamma} y_\gamma \quad (3.7)$$

and this represents the dynamics of the perturbation.

The system has a trivial translational invariance that reads

$$f_\alpha(x + z) = f_\alpha(x) \quad (3.8)$$

Indeed with a simultaneous drift z of all the probes nothing change in the system.

$f_\alpha(x + z)$ can be rewritten at first-order as

$$f_\alpha(x + z) = f_\alpha(x) + \sum_{\gamma} \frac{\partial f_\alpha(x)}{\partial x_\gamma} z_\gamma \quad (3.9)$$

where $z_\gamma = z$.

In order to satisfy eq. (3.8) for every z

$$\sum_{\gamma} \frac{\partial f_\alpha(x)}{\partial x_\gamma} = 0 \implies M_{\alpha\alpha} + \sum_{\gamma \neq \alpha} M_{\alpha\gamma} = 0 \quad (3.10)$$

Since the probes are identical and equidistant, the matrix elements with $\alpha \neq \gamma$ can be written as $M_{\alpha\gamma} = m_{\gamma-\alpha}$. These can be considered as effective non symmetric spring constants.

Can these spring constants be rewritten in function of parameters that depend on general features of the system? Let us try to derive a new form for these spring constants.

$$\begin{aligned} M_{\alpha\gamma} &= \frac{\partial f_\alpha(x)}{\partial x_\gamma} = -\frac{\partial}{\partial x_\gamma} \int_0^L \frac{\partial U(x, \eta)}{\partial x_\alpha} \rho_x(\eta) d\eta = \\ &= -\int_0^L \frac{\partial^2 U(x, \eta)}{\partial x_\gamma \partial x_\alpha} \rho_x(\eta) d\eta - \int_0^L \frac{\partial U(x, \eta)}{\partial x_\alpha} \frac{\partial \rho_x(\eta)}{\partial x_\gamma} d\eta \end{aligned} \quad (3.11)$$

Inserting the explicit expression of $\rho_x(\eta)$ we get

$$\begin{aligned}
M_{\alpha\gamma} &= - \int_0^L u''(x_\alpha - \eta) \delta_{\alpha\gamma} \rho_x(\eta) d\eta + \\
&- \int_0^L d\eta u'(x_\alpha - \eta) \left[\int_0^L \frac{\rho^0 L}{\Omega(x)} e^{-\beta W_x(\eta, \eta')} (-\beta) \frac{\partial(U(x, \eta) - U(x, \eta'))}{\partial x_\gamma} d\eta' + \right. \\
&+ \left. \frac{\partial}{\partial x_\gamma} \left(\frac{1}{\Omega(x)} \right) \int_0^L \rho^0 L e^{-\beta W_x(\eta, \eta')} d\eta' \right] = \\
&= - \int_0^L u''(x_\alpha - \eta) \delta_{\alpha\gamma} \rho_x(\eta) d\eta + \\
&+ \beta \int_0^L u'(x_\alpha - \eta) \int_0^L \frac{\rho^0 L}{\Omega(x)} e^{-\beta W_x(\eta, \eta')} u'(x_\gamma - \eta) d\eta' + \\
&- \beta \int_0^L u'(x_\alpha - \eta) \int_0^L \frac{\rho^0 L}{\Omega(x)} e^{-\beta W_x(\eta, \eta')} u'(x_\gamma - \eta') d\eta' + \\
&+ \int_0^L u'(x_\alpha - \eta) \frac{1}{\Omega^2(x)} \frac{\partial}{\partial x_\gamma} \Omega(x) \int_0^L \rho^0 L e^{-\beta W_x(\eta, \eta')} d\eta'
\end{aligned} \tag{3.12}$$

that can be rewritten as

$$\begin{aligned}
M_{\alpha\gamma} &= - \int_0^L u''(x_\alpha - \eta) \delta_{\alpha\gamma} \rho_x(\eta) d\eta + \beta \int_0^L u'(x_\alpha - \eta) u'(x_\gamma - \eta) \rho_x(\eta) d\eta + \\
&- \beta \int_0^L d\eta u'(x_\alpha - \eta) \int_0^L u'(x_\gamma - \eta') \mu_x(\eta, \eta') d\eta' + \\
&+ \frac{\partial}{\partial x_\gamma} \log \Omega(x) \int_0^L u'(x_\alpha - \eta) \rho_x(\eta) d\eta
\end{aligned} \tag{3.13}$$

If $\alpha \neq \gamma$ the first term vanishes and because of the probes' isolation condition also the second term vanishes.

Then, by translational invariance of the normalization factor ($\Omega(x+z) = \Omega(x)$) the condition

$$\sum_\gamma \frac{\partial \log \Omega(x)}{\partial x_\gamma} = 0 \tag{3.14}$$

is derived in an equivalent way of (3.10). In particular for the equidistant configuration this condition simplifies and becomes

$$\frac{\partial \log \Omega(x^*)}{\partial x_\gamma} = 0 \tag{3.15}$$

for each probe. This means that, for the equidistant configuration, also the last term in the expression for $M_{\alpha\gamma}$ vanishes.

Consequently, the expression of the matrix element for the equidistant configuration simplifies a lot

$$\begin{aligned}
M_{\alpha\gamma}(x^*) &= -\beta \int_0^L d\eta u'(x_\alpha - \eta) \int_0^L u'(x_\gamma - \eta') \mu_x(\eta, \eta') d\eta' & (3.16) \\
&= -\beta \frac{\rho^0 L}{\Omega(x^*)} \int_0^L d\eta \int_\eta^{\eta+L} d\eta' u'(x_\alpha^* - \eta) u'(x_\gamma^* - \eta') e^{-\beta[U(x^*, \eta) - U(x^*, \eta') + \varepsilon(\eta' - \eta)]} \\
&= -\beta \frac{\rho^0 L}{\Omega(x^*)} \int_0^L d\eta \int_\eta^{\eta+L} d\eta' u'(\eta - x_\alpha^*) u'(\eta' - x_\gamma^*) e^{-\beta[U(x^*, \eta) - U(x^*, \eta') + \varepsilon(\eta' - \eta)]} \\
&= -\beta \frac{\rho^0 L}{\Omega(x^*)} \int dz \int dz' u'(z) u'(z') e^{-\beta[u(z) - u(z') + \varepsilon(z' - z) + \varepsilon(x_\alpha^* - x_\gamma^*)]} \\
&= -\beta \frac{\rho^0 L}{\Omega(x^*)} I^+ I^- e^{-\beta\varepsilon(x_\gamma^* - x_\alpha^*)}
\end{aligned}$$

where $I^\pm = \int_{-\delta}^\delta dz u'(z) e^{\pm[\beta u(z) - \beta\varepsilon z]}$. In particular

$$\begin{aligned}
I^- &= \int_{-\delta}^\delta dz u'(z) e^{-\beta u(z) + \beta\varepsilon z} = \frac{-\beta}{-\beta} \int_{-\delta}^\delta dz (u'(z) - \varepsilon) e^{-\beta u(z) + \beta\varepsilon z} + \int_{-\delta}^\delta dz \varepsilon e^{-\beta u(z) + \beta\varepsilon z} = \\
&= -\frac{1}{\beta} \left[e^{-\beta u(\delta) + \beta\varepsilon\delta} - e^{-\beta u(-\delta) - \beta\varepsilon\delta} \right] + \varepsilon \int_{-\delta}^\delta dz e^{-\beta u(z) + \beta\varepsilon z} = \\
&= -\int_{-\delta}^\delta dz e^{\beta\varepsilon z} + \varepsilon \int_{-\delta}^\delta dz e^{-\beta u(z) + \beta\varepsilon z} = \varepsilon \int_{-\delta}^\delta e^{\beta\varepsilon z} \phi^-(z) dz \\
&= \varepsilon B^- & (3.17)
\end{aligned}$$

and analogously $I^+ = -\varepsilon B^+$.

Therefore the spring constants for the equidistant configuration are

$$M_{0\alpha} = m_\alpha = \frac{\beta \rho^0 L}{\Omega(x^*)} \varepsilon^2 B e^{-\beta\varepsilon x_\alpha^*} = \frac{\zeta j^* B}{l_d^2 (1 - e^{-\frac{L}{l_d}})} e^{-\frac{L}{N l_d} \alpha} \quad (3.18)$$

that, in order to simplify the notation, can just be written as

$$m_\alpha = D e^{-\xi \alpha} \quad (3.19)$$

where $D = \frac{\beta \varepsilon^2 \rho^0 L B}{\Omega(x^*)}$ and $\xi = \frac{\beta \varepsilon L}{N}$.

In the globally strong driving regime, in which $l_d \ll L$, D can be written also as

$$D = \frac{\beta^2 \varepsilon^3 \rho^0 B}{Z(x^*)} \quad (3.20)$$

Indeed from (2.27)

$$\frac{\beta^2 \varepsilon^3 \rho^0 B}{Z(x^*)} = \frac{\beta^2 \varepsilon^3 \rho^0 B L}{\beta \varepsilon \Omega(x^*)} (1 - e^{-\beta \varepsilon L}) \quad (3.21)$$

and for $l_d \ll L$

$$\frac{\beta^2 \varepsilon^3 \rho^0 B}{Z(x^*)} = \frac{\beta \varepsilon^2 \rho^0 B L}{\Omega(x^*)} = D \quad (3.22)$$

Let us go back now to the linearized dynamics of the perturbation and write it in a different form.

$$\Gamma y_\alpha = \sum_{\gamma} M_{\alpha\gamma} y_\gamma = \sum_{\gamma=1}^{N-1} m_\gamma (y_{\alpha+\gamma} - y_\alpha) \quad (3.23)$$

Indeed

$$\begin{aligned} \sum_{\gamma} M_{\alpha\gamma} y_\gamma &= M_{\alpha\alpha} y_\alpha + \sum_{\gamma \neq \alpha} m_{\gamma-\alpha} y_\gamma \\ &= M_{\alpha\alpha} y_\alpha + \sum_{\gamma=1}^{N-1} m_\gamma y_{\alpha+\gamma} \end{aligned} \quad (3.24)$$

$$\begin{aligned} \text{from condition (3.10)} &= M_{\alpha\alpha} y_\alpha + \sum_{\gamma=1}^{N-1} m_\gamma y_{\alpha+\gamma} - y_\alpha \left(M_{\alpha\alpha} + \sum_{\gamma=1}^{N-1} m_\gamma \right) \\ &= \sum_{\gamma=1}^{N-1} m_\gamma (y_{\alpha+\gamma} - y_\alpha) \end{aligned}$$

From equation (3.23) it is easy to see that the zero mode $Y = \sum_{\alpha} y_\alpha$ is conserved.

In particular on the invariant hypersurface $Y = 0$ the configuration $y_\alpha \equiv 0$ is stable for $B > 0$. In order to prove that Lyapunov functions will be used.

Let us quickly recall the concept of Lyapunov function within Lyapunov stability theory [15].

Given a dynamical system

$$\dot{x} = f(x, t) \quad x = (x_1, \dots, x_n) \in \mathbb{R}^n \quad (3.25)$$

and a fixed point x_0 such that

$$f(x_0, t) = 0 \quad (3.26)$$

where $f : U \times \mathbb{R}^+ \rightarrow \mathbb{R}^n$ is a continuous function with continuous first derivatives x .

A scalar function $V : U \rightarrow \mathbb{R}$ is a Lyapunov function if:

- $V(x) > 0$ for $x \neq x_0$,
- $V(x_0) = 0$ and

$$\bullet \nabla V(x) \cdot f(x) = \frac{\partial}{\partial x_1} V(x) f_1(x) + \dots + \frac{\partial}{\partial x_n} V(x) f_n(x) \leq 0$$

The Lyapunov lemma states that if such a function V exists, the fixed point x_0 is Lyapunov-stable.

From the dynamics described by equation 3.23 it is clear that $y_\alpha \equiv 0$ is a fixed point.

Consider the function

$$\Lambda(y) = \frac{1}{2\Gamma} \sum_{\alpha} y_{\alpha}^2 \quad (3.27)$$

$\Lambda(y)$ is always positive except for $y \equiv 0$ where it is 0. Its derivative

$$\begin{aligned} \dot{\Lambda}(y) &= \sum_{\alpha} \dot{y}_{\alpha} y_{\alpha} = \sum_{\alpha} \sum_{\gamma=1}^{N-1} m_{\gamma} (y_{\alpha+\gamma} - y_{\alpha}) y_{\alpha} \\ &= \sum_{\gamma=1}^{N-1} m_{\gamma} \sum_{\alpha=0}^{N-1} y_{\alpha} (y_{\alpha+\gamma} - y_{\alpha}) = -\frac{1}{2} \sum_{\gamma=1}^{N-1} m_{\gamma} \sum_{\alpha=0}^{N-1} (y_{\alpha+\gamma} - y_{\alpha}) (y_{\alpha+\gamma} - y_{\alpha}) \end{aligned} \quad (3.28)$$

is always ≤ 0 . Hence $\Lambda(y)$ is a Lyapunov function and $y \equiv 0$ is Lyapunov-stable.

Having proved the mechanical stability of the equidistant configuration, in the next chapter the relaxation of an initial perturbation to such a stationary configuration will be studied.

Chapter 4

Relaxation to the crystal pattern

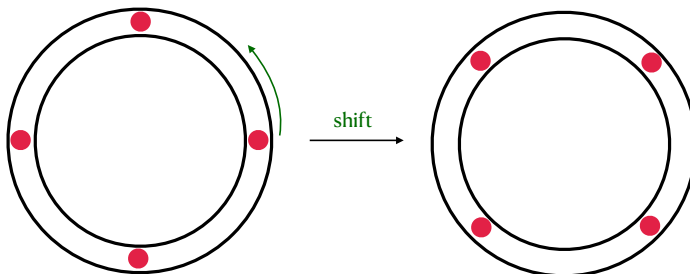
The linear dynamics of (small) deviations y_α is then

$$\Gamma \dot{y}_\alpha = \sum_{\gamma=1}^{N-1} m_\gamma (y_{\alpha+\gamma} - y_\alpha) \quad (4.1)$$

for which the zero mode $Y := \sum_\alpha y_\alpha$ is conserved.

The goal of this chapter is to solve (4.1) and see if such an equation leads to a relaxation towards a crystal-like pattern for the probes.

Setting $\sum_\alpha y_\alpha = \kappa$, if the crystal pattern is effectively reached, the perturbations from the equidistant configuration are expected to be equal for all the probes. Indeed, having for all the probes the same deviation from the equidistant configuration means that the probes are still equidistant. An equal shift of all the particles of a crystal maintains the equidistance of such particles in the system (see figure below where each *red* probe is shifted by the same *green* shift).



At the end it is expected for each probe to have

$$y_\alpha(t) \rightarrow \frac{\kappa}{N} \quad (4.2)$$

in the large time limit, so that all the $y_\alpha(t)$ are the same and $\sum_\alpha y_\alpha$ is conserved.

Let us start by solving directly two simple cases, with 2 and 3 probes respectively.

4.1 The case with 2 and 3 probes

4.1.1 System of 2 probes

$$\begin{cases} \Gamma \dot{y}_0 = m_1(y_1 - y_0) \\ \Gamma \dot{y}_1 = m_1(y_0 - y_1) \end{cases} \quad \text{where } y_0 + y_1 = \kappa$$

Using the zero mode conservation the system can be reduced to a single differential equation

$$\dot{y}_0 + \frac{2m_1}{\Gamma} y_0 = \frac{m_1}{\Gamma} \kappa \quad (4.3)$$

which solution is known:

$$\begin{aligned} y_0(t) &= e^{-\frac{2m_1}{\Gamma}t} \left[y_0(0) + \int_0^t \frac{m_1 \kappa}{\Gamma} e^{\frac{2m_1 s}{\Gamma}} ds \right] \\ &= e^{-\frac{2m_1}{\Gamma}t} \left[y_0(0) + \frac{\kappa}{2} (e^{\frac{2m_1}{\Gamma}t} - 1) \right] \\ &= e^{-\frac{2m_1}{\Gamma}t} \left[y_0(0) - \frac{\kappa}{2} \right] + \frac{\kappa}{2} \xrightarrow{t \rightarrow \infty} \frac{\kappa}{2} \end{aligned} \quad (4.4)$$

From this $y_1(t)$ follows as

$$y_1(t) = \kappa - y_0(t) \xrightarrow{t \rightarrow \infty} \frac{\kappa}{2} \quad (4.5)$$

Both probes for large times, tend to $\frac{\kappa}{2}$, as expected.

4.1.2 System of 3 probes

For $N=3$ the system of differential equations is

$$\begin{cases} \Gamma \dot{y}_0 = m_1(y_1 - y_0) + m_2(y_2 - y_0) \\ \Gamma \dot{y}_1 = m_1(y_2 - y_1) + m_2(y_0 - y_1) \\ \Gamma \dot{y}_2 = m_1(y_0 - y_2) + m_2(y_1 - y_2) \end{cases} \quad \text{where } y_0 + y_1 + y_2 = \kappa$$

The system can be reduced to a single second order differential equation of the form

$$\ddot{y}_1 + A\dot{y}_1 + By_1 = C$$

where

$$A = \frac{3(m_1 + m_2)}{\Gamma}, \quad B = \frac{3(m_1^2 + m_2^2 + m_1 m_2)}{\Gamma^2}, \quad C = \frac{\kappa(m_1^2 + m_2^2 + m_1 m_2)}{\Gamma^2}$$

Finding the homogeneous and particular solutions of the equation at the end the solution for $y_1(t)$ is

$$y_1 = e^{-\frac{3(m_1+m_2)}{2\Gamma}t} \left[c_1 \cos\left(\frac{\sqrt{3}}{2} \frac{(m_1 - m_2)}{\Gamma} t\right) + c_2 \sin\left(\frac{\sqrt{3}}{2} \frac{(m_1 - m_2)}{\Gamma} t\right) \right] + \frac{\kappa}{3} \quad (4.6)$$

that tends to $\frac{\kappa}{3}$ for $t \rightarrow \infty$ and it is trivial to show that also y_0 and y_2 tend to $\frac{\kappa}{3}$.

These two simple examples are in agreement with the idea of equation (4.2) but obviously this is not enough.

The next section gives a different and surprising approach to the study of the dynamics, through the use of a Compound Poisson Process.

4.2 Dynamics as a Compound Poisson Process

The idea is to construct a particular compound poisson process in a way that can be useful to study the system's dynamics.

Consider the random variable \mathcal{J} having distribution $\mathbf{P}[\mathcal{J} = \alpha] = (e^\xi - 1)e^{-\xi\alpha}$. The momenta can be computed as

$$\langle \mathcal{J} \rangle = (e^\xi - 1) \sum_{\alpha} \alpha e^{-\xi\alpha} = (1 - e^\xi) \frac{\partial}{\partial \xi} \left(\frac{1}{1 - e^{-\xi}} \right) = \frac{1}{1 - e^{-\xi}}$$

$$\langle \mathcal{J}^2 \rangle = (e^\xi - 1) \sum_{\alpha} \alpha^2 e^{-\xi\alpha} = (e^\xi - 1) \frac{\partial^2}{\partial \xi^2} \frac{1}{1 - e^{-\xi}} = \frac{1 + e^{-\xi}}{(1 - e^{-\xi})^2}$$

Recalling that, for $\alpha \neq 0$,

$$m_\alpha = D e^{-\xi\alpha} \quad (4.7)$$

where $D = \frac{\beta \varepsilon^2 \rho^0 L B}{\Omega(x^*)}$ and $\xi = \frac{\beta \varepsilon L}{N}$, allows to rewrite

$$\sum_{\gamma > 0} m_\gamma = D \sum_{\gamma > 0} e^{-\xi\gamma} = D \left[\frac{1}{1 - e^{-\xi}} - 1 \right] = \frac{D}{e^\xi - 1}. \quad (4.8)$$

$P[J = \alpha] = (e^\xi - 1) e^{-\xi\alpha}$ can then be rewritten as

$$\mathbf{P}[J = \alpha] = \frac{m_\alpha}{\sum_{\gamma>0} m_\gamma} \quad (4.9)$$

and so the probabilities are proportional to m_α .

The compound Poisson process can then be constructed by taking independent copies \mathcal{J}_i of \mathcal{J} to make the random variable

$$\mathcal{X}(t) = \sum_{i=1}^{N(t)} \mathcal{J}_i \quad (4.10)$$

where $N(t)$ is a Poisson process with rate Λ ,

$$\Lambda = \frac{1}{\Gamma} \sum_{\gamma>0} m_\gamma = \frac{D}{\Gamma} \frac{1}{e^\xi - 1}, \quad \text{for some } \Gamma > 0.$$

$\mathcal{X}(t)$ is then a discrete *compound Poisson process*, takes values in $\mathbb{N} = \{0, 1, 2, \dots\}$ and starts from $\mathcal{X}(0) = 0$.

The time-dependent probabilities for such a process to have a particular values ($p_\alpha(t) = \mathbf{P}[\mathcal{X}(t) = \alpha]$) satisfy a Master equation. That is because at rate Λ a random variable \mathcal{J} is added to the sum. In particular the rates of the transitions are

$$k(\alpha, \alpha + \gamma) = \Lambda \mathbf{P}[J = \gamma] = m_\gamma / \Gamma$$

for $\alpha = 0, \dots, N-1 \pmod{N}$ and $\gamma = 1, \dots, N-1$. Other types of transitions are forbidden ($p_\alpha \equiv 0$ whenever $\alpha < 0$).

Then, the master equation for $p_\alpha(t)$ is

$$\begin{aligned} \dot{p}_\alpha &= \sum_{\gamma>0} [p_{\alpha-\gamma} k(\alpha-\gamma, \gamma) - p_\alpha k(\alpha, \alpha+\gamma)] \\ &= \frac{1}{\Gamma} \sum_{\gamma>0} m_\gamma [p_{\alpha-\gamma} - p_\alpha]. \end{aligned} \quad (4.11)$$

By replacing α with $-\alpha$ it gets the form

$$\dot{p}_{-\alpha} = \frac{1}{\Gamma} \sum_{\gamma>0} m_\gamma [p_{-(\alpha+\gamma)} - p_{-\alpha}], \quad \alpha = 0, -1, -2, \dots \quad (4.12)$$

It is clear from equation (4.1) that the $y_\alpha(t)$, $\alpha = 0, -1, -2, \dots \pmod{N}$, solve a similar problem on the ring (now running in the opposite direction). More precisely,

$$\begin{aligned} y_{-\alpha}(t) &= \kappa \sum_{k=0}^{+\infty} p_{\alpha+kN}(t), \quad \alpha = 0, 1, \dots, N-1 \\ &= \kappa \mathbf{P}[\mathcal{X}(t) = \alpha \pmod{N}] \end{aligned} \quad (4.13)$$

The solution to the linearized probe dynamics can then be obtained via solving the compound Poisson process $\mathcal{X}(t)$.

In particular from standard results on Poisson processes ([10]) we obtain

$$p_0(t) = \mathbf{P}[\mathcal{X}(t) = 0] = \frac{(\Lambda t)^0}{0!} e^{-\Lambda t} = e^{-\Lambda t} = e^{-\frac{Dt}{e^\xi - 1}} \quad (4.14)$$

that is just the probability for the Poisson process of not having jumped yet at time t .

$$\langle \mathcal{X}(t) \rangle = \langle \mathcal{J} \rangle \Lambda t = \frac{e^\xi}{(e^\xi - 1)^2} \frac{Dt}{\Gamma} \quad (4.15)$$

$$\text{Var} \mathcal{X}(t) = \langle \mathcal{J}^2 \rangle \Lambda t = \frac{e^\xi(e^\xi + 1)}{(e^\xi - 1)^3} \frac{Dt}{\Gamma} \quad (4.16)$$

Indeed, for (4.15)

$$\langle \mathcal{X}(t) \rangle = \left\langle \sum_{i=1}^{N(t)} \frac{1}{1 - e^{-\xi}} \right\rangle = \frac{1}{1 - e^{-\xi}} \langle N(t) \rangle = \frac{\Lambda t}{1 - e^{-\xi}} = \frac{e^\xi}{(e^\xi - 1)^2} \frac{Dt}{\Gamma} \quad (4.17)$$

and for (4.16) the law of total variance should be used [20]. Such law states that, if X and Y are random variables on the same probability space, and the variance of Y is finite, then,

$$\text{Var}(Y) = E[\text{Var}(Y|X)] + \text{Var}(E[Y|X])$$

where $E[Z]$ is the expectation value of Z . So

$$\begin{aligned} \text{Var}(\mathcal{X}(t)) &= E[\text{Var}(\mathcal{X}(t)|N(t))] + \text{Var}(E[\mathcal{X}(t)|N(t)]) \quad (4.18) \\ &= E[N(t)\text{Var}(\mathcal{J})] + \text{Var}(N(t)E[\mathcal{J}]) \\ &= \text{Var}(\mathcal{J})E[N(t)] + \langle N(t)^2 E[\mathcal{J}]^2 \rangle - \langle N(t) E[\mathcal{J}] \rangle^2 \\ &= \text{Var}(\mathcal{J})E[N(t)] + E[\mathcal{J}]^2 \cdot \text{Var}N(t) \\ &= \text{Var}(\mathcal{J}) \cdot \Lambda t + E[\mathcal{J}]^2 \cdot \Lambda t = \Lambda t \cdot E[\mathcal{J}^2] \end{aligned}$$

and (4.16) follows from this.

From equations (4.14), (4.15) and (4.16) it is clear that the process $\mathcal{X}(t)$ leaves the origin and on average moves with speed $\langle \mathcal{J} \rangle \Lambda$ while diffusing. Then, by correspondence (4.13), the initial perturbation y starts from the first probe, decays exponentially fast and moves in the negative direction (with respect to the driven force). It reaches again the first probe and so on until it spreads over the whole circle. It is then possible to detect three *a priori* different times scales:

(I) the characteristic time of initial decay of the perturbation at the origin (from 4.14),

$$\tau_0 = \frac{1}{\Lambda} = \frac{\Gamma}{\sum_{\alpha=1}^{N-1} m_\alpha} = \frac{\Gamma}{D}(e^\xi - 1) \quad (4.19)$$

(II) the period of the *echo effect*, after which the Poisson wave visits the origin, (from 4.15),

$$\tau_{\text{echo}} = \frac{N}{\langle J \rangle \Lambda} = \frac{(e^\xi - 1)^2}{e^\xi} \frac{\Gamma N}{D} \quad (4.20)$$

(III) the relaxation time defined as a characteristic time in which the wave spreads over the whole circle, (from 4.16),

$$\tau_{\text{relax}} = \frac{N^2}{\langle J^2 \rangle \Lambda} = \frac{(e^\xi - 1)^3}{e^\xi(e^\xi + 1)} \frac{\Gamma N^2}{D} \quad (4.21)$$

Whenever $N \gg 1$ the three time scales are well separated, in the sense that

$$\tau_0 \ll \tau_{\text{echo}} \ll \tau_{\text{relax}}$$

and this means that these are localized distinct time scales which are all relevant in the description of the relaxation of a local perturbation to the crystal patterns.

The three time scales, in particular, will be detected in the following analysis.

4.3 Strong driving regime approximation of the elastic constants

Rewriting the expression for the elastic constants that was derived in (3.18)

$$m_\alpha = \frac{\zeta j^* B}{l_d^2 (1 - e^{-\frac{L}{N l_d}})} e^{-\frac{L}{N l_d} \alpha} \quad (4.22)$$

it is possible to analyse it for different nonequilibrium regimes.

In particular, for globally weakly driven colloids ($L \ll l_d$), the exponential damping of m_α in α is negligible and the elastic constants become almost homogeneous.

Instead, in the globally strong driving regime ($L \gg l_d$), the m_α exhibit total asymmetry as $m_{N-\alpha}$ becomes negligible for $1 \leq \alpha \ll N$. In general m_α is negligible whenever the distance $\alpha \frac{L}{N}$ between the probes 0 and α is large compared to the driving length scale l_d .

It seems then reasonable and in agreement with the strong driving regime approximation to consider just m_1 as relevant ($m_\alpha = \delta_{\alpha,1}m_1$) in the perturbation dynamics and to rewrite equation (4.1) as

$$\Gamma \dot{y}_\alpha = m_1(y_{\alpha+1} - y_\alpha) \quad (4.23)$$

This equation can further be simplified by rescaling time by $\tau_0 = \Gamma/m_1$. In this way equation (4.23) becomes

$$\dot{y}_\alpha = y_{\alpha+1} - y_\alpha \quad (4.24)$$

This is a much simpler equation to solve and in particular the idea is to try to solve it by using the ansatz

$$y_\alpha(t) = e^{-t} f_\alpha(t) \quad (4.25)$$

Inserting (4.25) in (4.24) it is easy to find

$$\dot{f}_\alpha = f_{\alpha+1} \quad (4.26)$$

that is a matrix equation $\dot{f} = Af$ where A is the $N \times N$ clock-and-shift matrix

$$A = \begin{pmatrix} 0 & 1 & 0 & \cdots & 0 \\ 0 & 0 & 1 & \ddots & \vdots \\ \vdots & \vdots & 0 & \ddots & 0 \\ 0 & \vdots & \vdots & \ddots & 1 \\ 1 & 0 & \cdots & \cdots & 0 \end{pmatrix} \quad (4.27)$$

That matrix has eigenvalues

$$\lambda_k = e^{2\pi i k/N}, \quad k = 1, \dots, N \quad (4.28)$$

and respective eigenvectors

$$u_{\alpha,k} = e^{2\pi i k \alpha/N} \quad (4.29)$$

Indeed,

$$u_{\alpha+1,k} = e^{2\pi i k/N} e^{2\pi i k \alpha/N} \quad (4.30)$$

The solution is therefore

$$f_\alpha = \sum_k c_k e^{2\pi i k \alpha/N} e^{\lambda_k t} \quad (4.31)$$

In order to find easily an explicit solution, a particular set of initial conditions is assumed. Each probe is assumed to have a null initial perturbation from the equidistant configuration except the probe 0, for which $y_0(0) = \kappa$.

This assumption seems strong but actually it is not relevant for the general trend of the system's relaxation and this will be analysed later.

This particular set of initial conditions is translated into the relation

$$\sum_k c_k e^{2\pi i k \alpha / N} = \kappa \delta_{\alpha,0} \quad (4.32)$$

and by the unitarity of the $u_{\alpha,k}$ -matrix, rows are orthogonal and we can take $c_k = \kappa/N$. The solution (in complex plane) of (4.24) is therefore

$$y_\alpha(t) = \frac{\kappa}{N} \sum_k e^{2\pi i k \alpha / N} e^{(\lambda_k - 1)t} \quad (4.33)$$

The real part of $\lambda_k - 1$ is non-positive, indeed $\text{Re}(\lambda_k - 1) = \cos(2\pi \frac{k}{N}) - 1 \leq 0$ and is zero only for $k = N$. Therefore, it is easy to conclude from (4.33) that $y_\alpha(t) \rightarrow \kappa/N$ for all α , as expected.

Inserting (4.28), equation (4.33) becomes

$$y_\alpha(t) = \frac{\kappa}{N} + \sum_{k=1}^{N-1} e^{2\pi i k \frac{\alpha}{N}} \cdot e^{(\cos \frac{2\pi k}{N} + i \sin \frac{2\pi k}{N} - 1)t} \quad (4.34)$$

$$= \frac{\kappa}{N} + \sum_{k=1}^{N-1} e^{i(\frac{2\pi k \alpha}{N} + \sin(\frac{2\pi k}{N})t)} \cdot e^{-t(1 - \cos \frac{2\pi k}{N})} \quad (4.35)$$

Defining the relaxation times as

$$\tau_k = \frac{1}{1 - \cos(2\pi \frac{k}{N})}, \quad k = 1, \dots, N-1 \quad (4.36)$$

and taking just the real part, the solution becomes

$$y_\alpha(t) = \frac{\kappa}{N} + \frac{\kappa}{N} \sum_{k=1}^{N-1} \cos \left[2\pi \frac{k \alpha}{N} + \sin \left(2\pi \frac{k}{N} \right) t \right] e^{-t/\tau_k} \quad (4.37)$$

with initial condition $y_\alpha(0) = \kappa \delta_{\alpha,0}$.

Equation (4.37) can also be rewritten as

$$y_\alpha(t) = \frac{\kappa}{N} + \frac{\kappa}{N} \sum_{k=1}^{N-1} \cos \left[\frac{2\pi k}{N} (\alpha + v_k t) \right] e^{-t/\tau_k} \quad (4.38)$$

where

$$v_k = \frac{N}{2\pi k} \sin \frac{2\pi k}{N}, \quad k = 1, \dots, N-1 \quad (4.39)$$

is the velocity that the oscillatory part in each term shows.

Let us now compare equation (4.37) with the simple cases of 2 and 3 probes that were exactly solved before.

Considering $N=2$ and using (4.37) the result is

$$\begin{cases} y_0(t) = \frac{\kappa}{2} + \frac{\kappa}{2}e^{-2t} \\ y_1(t) = \frac{\kappa}{2} - \frac{\kappa}{2}e^{-2t} \end{cases}$$

In subsection 4.1.1 the result, using as initial condition $y_\alpha(0) = \kappa\delta_{\alpha 0}$, was

$$\begin{cases} y_0(t) = \frac{\kappa}{2} + \frac{\kappa}{2}e^{-2\frac{m_1}{\Gamma}t} \\ y_1(t) = \frac{\kappa}{2} - \frac{\kappa}{2}e^{-2\frac{m_1}{\Gamma}t} \end{cases}$$

These two results are equivalent, the first one has just the time rescaled by $\tau_0 = \Gamma/m_1$. Indeed for $N=2$, the approximation $m_\alpha = \delta_{\alpha,1}m_1$ obviously coincides with the exact solution.

For the case $N=3$, differently, equation (4.37) will be an approximate solution of the system.

In subsection 4.1.2 the exact solution for $y_1(t)$ was

$$y_1(t) = e^{-\frac{3(m_1+m_2)}{2\Gamma}t} \left[c_1 \cos\left(\frac{\sqrt{3}}{2}\frac{(m_1-m_2)}{\Gamma}t\right) + c_2 \sin\left(\frac{\sqrt{3}}{2}\frac{(m_1-m_2)}{\Gamma}t\right) \right] + \frac{\kappa}{3} \quad (4.40)$$

where c_1 and c_2 have to be fixed from initial conditions.

From (4.37) instead, with $y_\alpha(0) = \kappa\delta_{\alpha 0}$ and so $y_1(0) = 0$ as initial condition, the solution is

$$\begin{aligned} y_1(t) &= \frac{\kappa}{3}e^{-\frac{3}{2}t} \left[\cos\left(\frac{2\pi}{3} + \frac{\sqrt{3}}{2}t\right) \cos\left(\frac{4\pi}{3} - \frac{\sqrt{3}}{2}t\right) \right] + \frac{\kappa}{3} \\ &= \frac{\kappa}{3}e^{-\frac{3}{2}t} \left[-\cos\left(\frac{\sqrt{3}}{2}t\right) - \sqrt{3}\sin\left(\frac{\sqrt{3}}{2}t\right) \right] + \frac{\kappa}{3} \quad (4.41) \end{aligned}$$

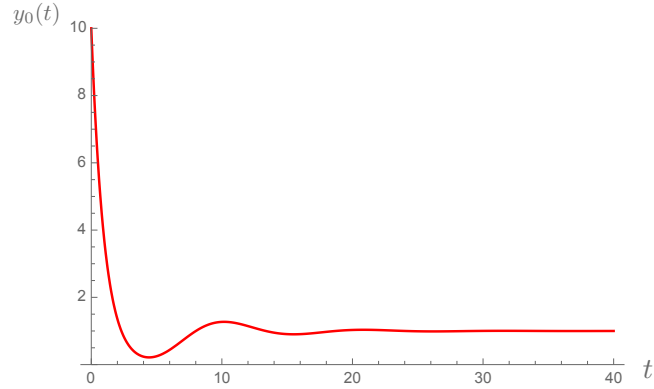
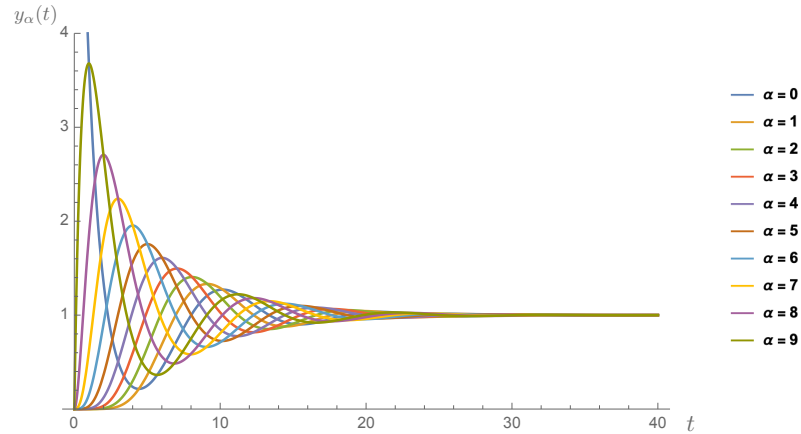
This is very similar to solution (4.40), but in this case m_2 is neglected and the time rescaled by $\tau_0 = \Gamma/m_1$.

Going now back to equation (4.37) it is possible to plot how $y_\alpha(t)$ varies with time, changing the probe α and the number of probes N .

In particular in all the plots the sum of initial perturbations will be fixed at $\kappa = 10$ a.u. and, considering an initial perturbation only on probe 0, the initial conditions will be $y_\alpha(0) = 10\delta_{\alpha,0}$ a.u. Remind also that the time is always rescaled by $\tau_0 = \Gamma/m_1$.

A first example is the plot of the trend of $y_0(t)$ for a system of 10 probes.

The trend is clear: the perturbation from the crystal configuration is 10 at $t=0$, then starts to oscillate and quickly reaches the expected value $\frac{\kappa}{N} = 1$.

Figure 4.1: $y_0(t)$ for a system with 10 probesFigure 4.2: $y_\alpha(t)$ evolution for a system with 10 probes

The same type of graph can be studied for the other 9 probes and, collecting all the trends in the same graph, figure (4.2) is obtained.

Qualitatively, it is possible to observe that all the probes' perturbations relax to the value $\frac{\kappa}{N} = 1$.

These graphs explicitly show the relaxation of the system (in this case of 10 probes) towards a crystal configuration.

4.3.1 Multi-probe initial conditions

This analysis that shows how the probes of a system relax to the crystal configuration was done by considering the initial condition

$$y_\alpha(0) = \kappa \delta_{\alpha,0} \quad (4.42)$$

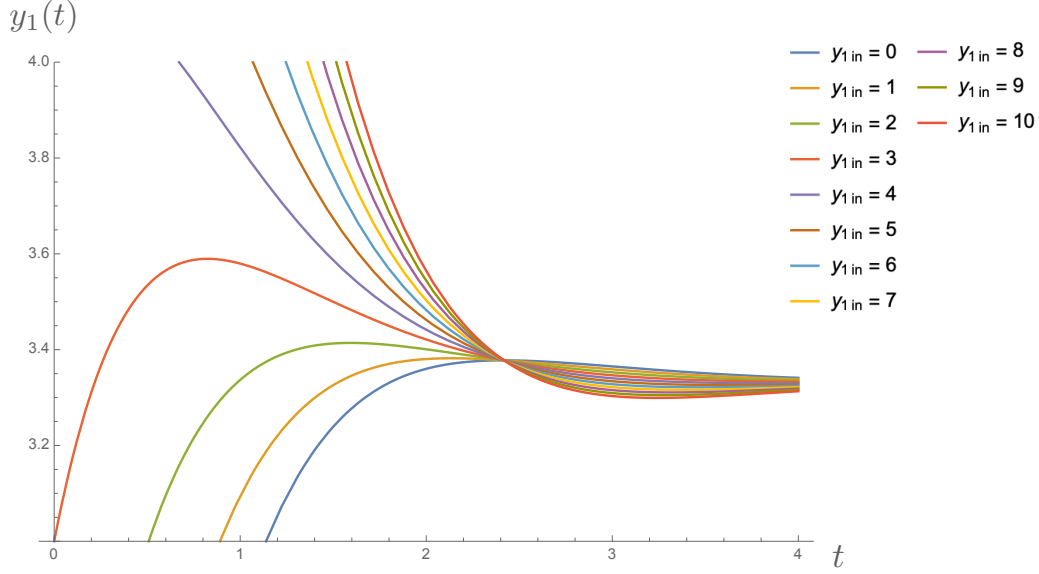


Figure 4.3: $y_1(t)$ for different values of initial conditions

that simply means that all the probes at $t=0$ are in their equidistant position, except probe 0 that has an initial perturbation equal to κ .

It is reasonable to think that initial conditions do not significantly change the relaxation towards the crystal pattern and so considering (4.42) as initial condition is just the simplest way to study the system.

In this part some trends of the probes' relaxation in the case of initial conditions different from eq. (4.42) will be shown.

Consider for example the case with 3 probes. From eq. (4.6) it is known that the evolution of the perturbation $y_1(t)$ is of the form

$$y_1(t) = e^{-\frac{3}{2\Gamma}(m_1+m_2)t} \left[c_1 \cos \left(\frac{\sqrt{3}}{2} \frac{(m_1 - m_2)}{\Gamma} t \right) + c_2 \sin \left(\frac{\sqrt{3}}{2} \frac{(m_1 - m_2)}{\Gamma} t \right) \right] + \frac{\kappa}{3} \quad (4.43)$$

and just from this expression is clear that the relaxation $y_1(t) \rightarrow \frac{\kappa}{3}$ does not depend on the coefficients c_1 and c_2 , fixed by the initial conditions.

Anyway let us again simplify the problem by considering consider $m_1 = 1$ and $m_2 = 0$. The difference is that now the initial perturbations $y_{0,in}$ and $y_{1,in}$ vary ($y_{2,in} = 0$ is instead fixed).

Considering always $\kappa = 10$ as sum of the perturbations, in figure 4.3 are the trends of $y_1(t)$ for different initial conditions. In the legends there is only the initial value of $y_{1,in}$ but obviously $y_{0,in} = 10 - y_{1,in}$.

It is clear that the evolution of $y_1(t)$ does not change significantly changing initial conditions. The trends are obviously different at the beginning,

for small t , but then $y_1(t)$ relaxes in the same way towards the asymptotic perturbation.

The same reasoning used for a system of 3 probes can be used also for any number of probes. Again, the only difference is for small times for which the initial conditions are relevant, but after that the trend of the relaxation is the same, no matter which are the initial conditions.

In order to make this argument more rigorous the *continuous dependence on the initial conditions theorem* can be used [8].

The theorem states that, given the Cauchy problem

$$\begin{cases} y' = f(t, y) \\ y(t_0) = y_0 \end{cases}$$

if $f : \Omega \subseteq \mathbb{R} \times \mathbb{R}^n \rightarrow \mathbb{R}^n$ is Lipschitz continuous (with respect to the variables y) in Ω , then:

- for each $(t_0, y_0), (t_0, z_0)$ there exist $\delta > 0$ and $C > 0$ such that

$$\sup_{t \in [t_0 - \delta, t_0 + \delta]} \|y(t; y_0) - y(t; z_0)\| \leq C \|y_0 - z_0\|$$

Since the assumption for the dynamics' linearization is the presence of small perturbations for the probes (and so also initial perturbations are small), it means that the theorem can be used to state that the solution does not depend a lot on initial conditions.

At the end it seems correct to simplify the problem and consider the total (initial) perturbation $\kappa = \sum_{\alpha} y_{\alpha}(0)$ concentrated on just one probe and all the other probes initially in the equidistant configuration, as done in all the previous analysis.

4.3.2 Time-scales

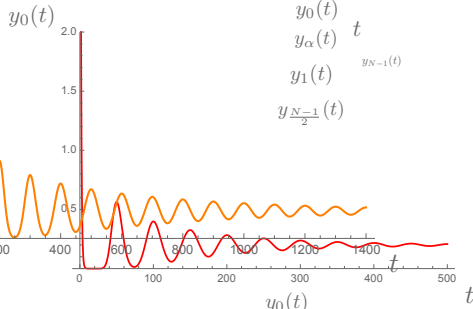
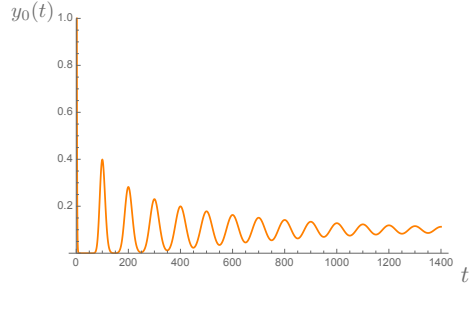
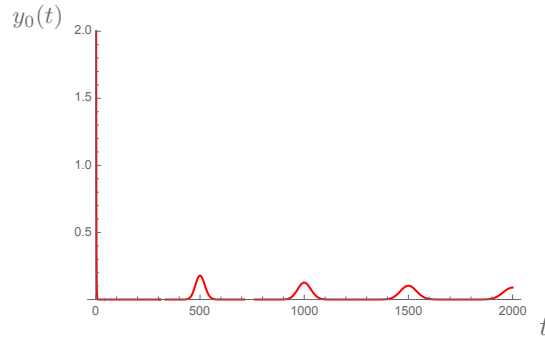
At the end of section 4.2, where a compound Poisson process description was used, some time scales were found as characteristic times of the relaxation. The following analysis will try to recognize such times in the perturbations' trends that come from equation (4.37).

The exponential decay with time of the peaks of the perturbations is clear from figure 4.2. The more interesting times and their dependence from N are the *echo-time* and the *relaxation time*.

The α can be fixed and it is possible to see how $y_{\alpha}(t)$ varies increasing N . In particular in the following graphs $\alpha = 0$ will be considered.

In figures 4.4, 4.5 and 4.6 it is immediate to notice how the peaks of the perturbations are at positions corresponding to $t = kN$ with $k = \{0, 1, 2, 3, \dots\}$. This is the appearance of the echo effect of equation (4.20), for which $\tau_{\text{echo}} \sim N$.

Graphs 4.7, 4.8, 4.9, 4.10 are then plots in which the variation in time of the perturbation of a fixed probe, for different N , is represented. Again the echo effect is clear.

Figure 4.4: $y_0(t)$ for $N=50$ Figure 4.5: $y_0(t)$ for $N=100$ Figure 4.6: $y_0(t)$ for $N=500$

In particular the perturbations are represented respectively for the first probe (figure 4.7), the second one (figure 4.8), the mid one (figure 4.9) and the last one (figure 4.10).

Let us now try to recognize in the graphs the relaxation time. In particular let us remind from equation (4.65) that

$$\tau_{\text{relax}} \sim N^2.$$

In figure 4.2 the relaxation of all the 10 probes was represented. The same graph can be done also for $N=20$ and $N=40$. Set $\tau_{\text{relax}10}$ as relaxation time for $N=10$, the expected relaxation times for $N=20$ and $N=40$ will be respectively $4\tau_{\text{relax}10}$ and $16\tau_{\text{relax}10}$ because of the dependence on N^2 .

Figures 4.11 and 4.12 represent the relaxation toward the asymptotic y_α for $N=20$ and $N=40$.

From figure 4.2 it is possible to identify $\tau_{\text{relax}10} \simeq 30$ (the unit of measure is seconds times the unit of measure of $\frac{m_1}{T}$) as the time at which all the probes have relaxed to the asymptotic value $\frac{k}{N}$. From graphs 4.11 and 4.12 it is clear that the relaxation times for $N=20$ and $N=40$ are really around $4\tau_{\text{relax}10}$ and $16\tau_{\text{relax}10}$, as expected.

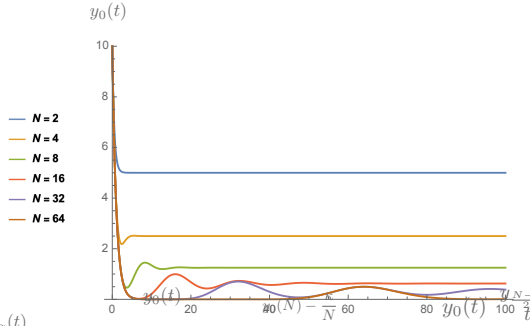


Figure 4.7: $y_0(t)$ for $N=2, 4, 8, 16, 32, 64$.

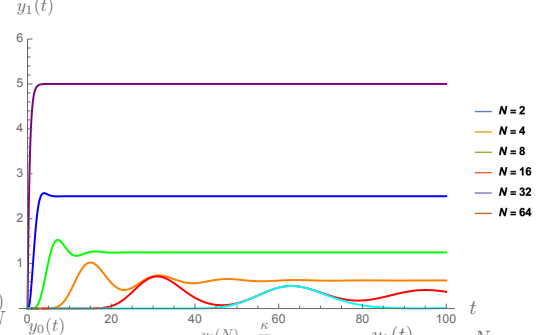


Figure 4.8: $y_1(t)$ for $N=2, 4, 8, 16, 32, 64$.

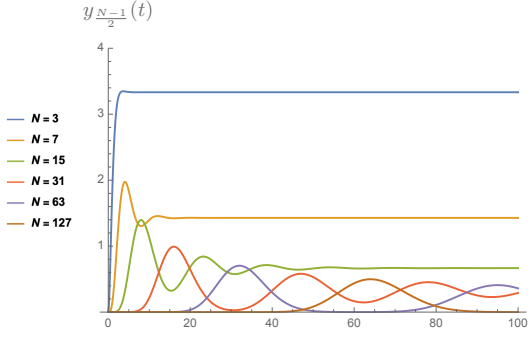


Figure 4.9: $y_{\frac{N-1}{2}}(t)$ for $N=3, 7, 15, 31, 63, 127$.

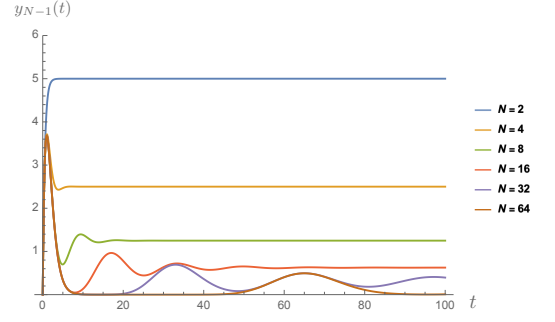


Figure 4.10: $y_{N-1}(t)$ $N=2, 4, 8, 16, 32, 64$.

In order to make the explanation of the N^2 -behaviour of τ_{relax} more rigorous, let us fix a threshold under which we consider the relaxation completed.

Let us concentrate only on the peaks (those that appear at time $t = kN$) of the graphs of $y_0(t)$ and see at which time their distance from the asymptotic displacement reaches a particular fixed threshold.

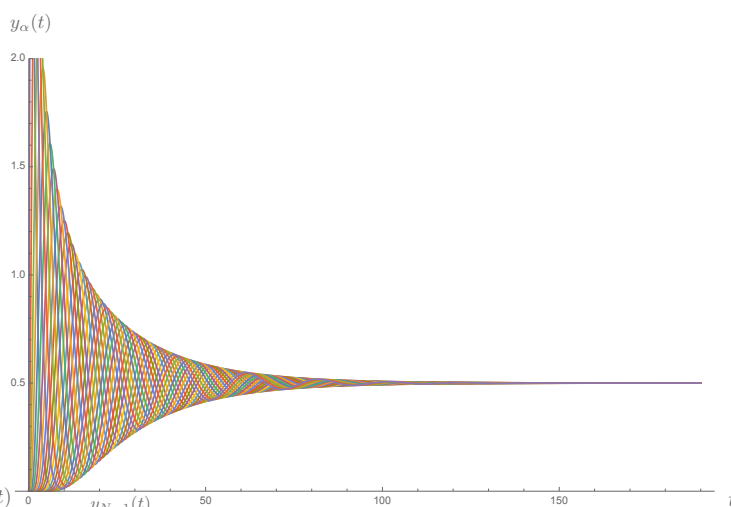
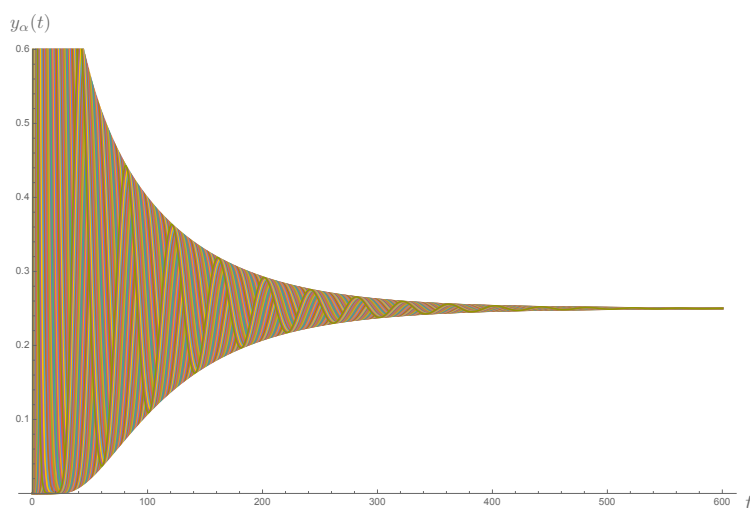
Let us for example fix a very low threshold at $y_0(t) - \frac{\kappa}{N} = 10^{-8}$ and see what happens for $N = 40, 80, 160$ (always with $\kappa = 10$).

The trends of $y_0(t) - \frac{\kappa}{N}$ for the three different N are shown in figures 4.13, 4.14 and 4.15.

Analyzing numerically at which time (τ_{thresh}) $y_0(t) - \frac{\kappa}{N}$ reaches the threshold, the result is

$$\tau_{\text{thresh}} = 1400 \quad \text{for } N=40 \quad \tau_{\text{thresh}} = 5540 \quad \text{for } N=80 \quad \tau_{\text{thresh}} = 22120 \quad \text{for } N=160$$

And this proves more rigorously the N^2 -dependence of the relaxation time.

Figure 4.11: $y_\alpha(t)$ evolution for a system with 20 probesFigure 4.12: $y_\alpha(t)$ evolution for a system with 40 probes

4.3.3 A natural ansatz for the Poisson process' master equation

Let us remind that the compound Poisson process is given by

$$\chi(t) = \sum_{i=1}^{N(t)} J_i \quad (4.44)$$

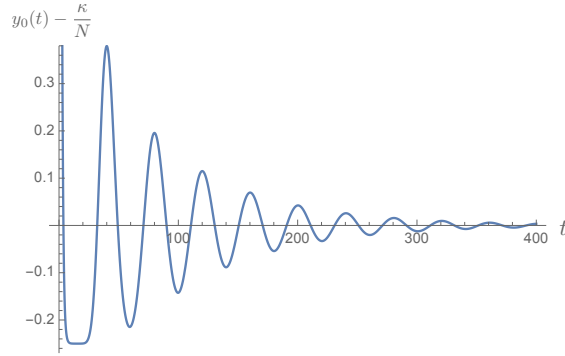


Figure 4.13: N=40

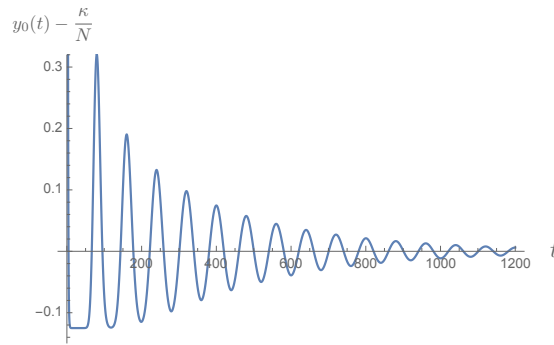


Figure 4.14: N=80

where $N(t)$ is a counting Poisson process.

Due to the fact that, considering only m_1 as different from 0, all the jumps J_i are equal to 1, the ansatz of our displacements from the equidistant configuration can also be chosen as

$$y_{N-\alpha}(t) = \kappa e^{-t} \sum_{k=0}^{\infty} \frac{t^{\alpha+Nk}}{(\alpha+Nk)!} \quad (4.45)$$

that is just a simple Poisson distribution. It is very simple to see how this form of the displacements solves the differential equation

$$\dot{y}_\alpha = y_{\alpha+1} - y_\alpha \quad (4.46)$$

(just plugging (4.45) in the equivalent equation $\dot{y}_{N-\alpha} = y_{N-\alpha+1} - y_{N-\alpha}$).

Let us see if, with this ansatz, also the condition $y_{N-\alpha}(t) \xrightarrow[t \rightarrow \infty]{} \frac{\kappa}{N}$ is satisfied $\forall \alpha$.

In order to do that it should be verified that

$$e^{-t} \sum_{k=0}^{\infty} \frac{t^{\alpha+Nk}}{(\alpha+Nk)!} \xrightarrow[t \rightarrow \infty]{} \frac{1}{N} \quad (4.47)$$

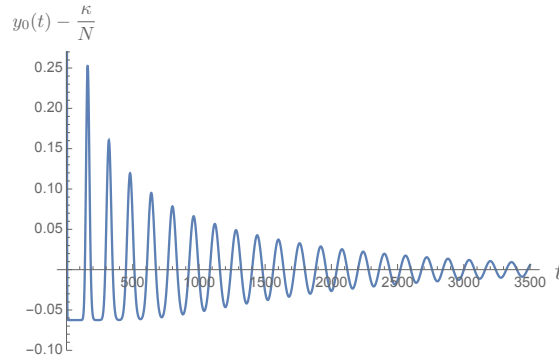


Figure 4.15: N=160

In the following calculations this is done for $\alpha = 0$ but the reasoning is the same also for $\alpha \neq 0$.

Let us consider the following equivalence

$$1 = e^{-t} e^t = e^{-t} \left[\left(1 + \frac{t^N}{N!} + \frac{t^{2N}}{(2N)!} + \frac{t^{3N}}{(3N)!} + \dots \right) + \left(\frac{t^{N-1}}{(N-1)!} + \frac{t^{2N-1}}{(2N-1)!} + \dots \right) + \left(\frac{t^{N-2}}{(N-2)!} + \dots \right) + \dots \right. \\ \left. \dots + \left(\frac{t^{N-(N-1)}}{1} + \frac{t^{2N-(N-1)}}{(N+1)!} + \dots \right) \right] \quad (4.48)$$

Inside the square brackets we have N groups of terms. Let us consider the first one multiplied by e^{-t} in the limit $t \rightarrow \infty$. Using De L'Hopital,

$$\lim_{t \rightarrow \infty} \frac{1 + \frac{t^N}{N!} + \frac{t^{2N}}{(2N)!} + \frac{t^{3N}}{(3N)!} + \dots}{e^t} = \lim_{t \rightarrow \infty} \frac{\frac{t^{N-1}}{(N-1)!} + \frac{t^{2N-1}}{(2N-1)!} + \dots}{e^t} \quad (4.49)$$

The same reasoning can be used also for all the other terms. At the end each group of terms multiplied by e^{-t} is the same in the limit $t \rightarrow \infty$. Finally, using the fact that $e^{-t} e^t = 1$ (obviously also in the limit $t \rightarrow \infty$), the result is

$$\lim_{t \rightarrow \infty} e^{-t} \times \text{any group of terms} = \frac{1}{N} \quad (4.50)$$

and in particular

$$\lim_{t \rightarrow \infty} e^{-t} \sum_{k=0}^{\infty} \frac{t^{Nk}}{(Nk)!} = \frac{1}{N} \quad (4.51)$$

The ansatz (4.45) seems a good ansatz in order to solve the linearized dynamics. In particular it is the natural ansatz to solve the master equation (4.12) for the probability of the Poisson Process.

Anyway, the visualization of periodicity on the probes of the ring it is not immediate for such an ansatz. In addition, the matrix equation analysis

(see equations 4.26 and 4.27) is definitely better usable in the case, that will be analysed later, for which more *elastic constants* m_γ are considered.

For these reasons, at the end, it seems reasonable to consider the analysis that lead to equation (4.37) as the most convenient one.

4.3.4 Contribution of all the elastic constants m_γ

In order to get to the dynamics' equation (4.23), it was assumed that m_1 could be considered as the only relevant *elastic constant*.

Now the analysis will be extended also in the case of the presence of all the m_γ 's.

In this case the dynamics' equation (with the time always rescaled by the factor $\frac{m_1}{\Gamma}$) has the form

$$\dot{y}_\alpha = y_{\alpha+1} - y_\alpha + \frac{m_2}{m_1}(y_{\alpha+2} - y_\alpha) + \frac{m_3}{m_1}(y_{\alpha+3} - y_\alpha) + \dots \quad (4.52)$$

Again the ansatz

$$y_\alpha(t) = e^{-t} f_\alpha(t) \quad (4.53)$$

can be used to easily get

$$\dot{f}_\alpha = f_{\alpha+1} + \frac{m_2}{m_1}(f_{\alpha+2} - f_\alpha) + \frac{m_3}{m_1}(f_{\alpha+3} - f_\alpha) + \dots \quad (4.54)$$

that is the matrix equation

$$\dot{f} = A f \quad (4.55)$$

where, defining $a_m = \frac{m_m}{m_1}$,

$$A = \begin{pmatrix} -\sum_{m=2}^{N-1} a_m & 1 & a_2 & a_3 \cdots & a_{N-1} \\ a_{N-1} & -\sum_{m=2}^{N-1} a_m & 1 & \ddots & \vdots \\ \vdots & \vdots & -\sum_{m=2}^{N-1} a_m & \ddots & a_2 \\ a_2 & \vdots & \vdots & \ddots & 1 \\ 1 & a_2 & \cdots & \cdots & -\sum_{m=2}^{N-1} a_m \end{pmatrix} \quad (4.56)$$

This kind of matrix is called circulant matrix ([2]) and is defined as in the following.

A $n \times n$ circulant matrix is a matrix of the form

$$C = \begin{pmatrix} x_0 & x_1 & x_2 & x_3 \cdots & x_{n-1} \\ x_{n-1} & x_0 & x_1 & \ddots & \vdots \\ \vdots & \vdots & x_0 & \ddots & x_2 \\ x_2 & \vdots & \vdots & \ddots & x_1 \\ x_1 & x_2 & \cdots & \cdots & x_0 \end{pmatrix} \quad (4.57)$$

for which the normalized eigenvectors are the Fourier modes

$$v_j = \frac{1}{\sqrt{n}} \left(1, \omega^j, \omega^{2j}, \dots, \omega^{(n-1)j} \right), \quad j = 0, 1, \dots, n-1 \quad (4.58)$$

where $\omega = e^{\frac{2\pi i}{n}}$ is a primitive n -th root of unity.

The corresponding eigenvalues are given by

$$\lambda_j = \sum_{l=0}^{n-1} x_l \omega^{jl} \quad (4.59)$$

Equation 4.55 involves the circulant matrix 4.56. The solution of such an homogeneous differential equation is

$$f_\alpha = \frac{1}{N} \sum_{j=0}^{N-1} \omega^{\alpha j} e^{\lambda_j t} c_j, \quad \alpha = 0, 1, \dots, N-1 \quad (4.60)$$

where λ_j are the (time-independent) eigenvalues of A.

From 4.53

$$y_\alpha(t) = \frac{1}{N} \sum_{j=0}^{N-1} c_j e^{\frac{2\pi i}{N} \alpha j} e^{(\lambda_j - 1)t}, \quad \alpha = 0, 1, \dots, N-1 \quad (4.61)$$

The real part of $\lambda_j - 1$ is non-positive. Indeed from 4.59

$$\operatorname{Re}(\lambda_j - 1) = \left[\sum_{l=0}^{N-1} x_l \cos\left(2\pi \frac{jl}{N}\right) \right] - 1 = x_0 + \left[\sum_{l=1}^{N-1} x_l \cos\left(2\pi \frac{jl}{N}\right) \right] - 1 \quad (4.62)$$

Since for $l > 0$ we have $x_l > 0$, the maximum value of such an expression is when all the cosines are 1 and so when $j = 0$. In that case $\lambda_0 = \sum_{l=0}^{N-1} x_l$ and considering the entries x_l of matrix 4.56 $\lambda_0 = 1$. Therefore for every other $j \neq 0$ we have

$$\operatorname{Re}(\lambda_j - 1) < 0 \quad (4.63)$$

From 4.61 it is then possible to write

$$\begin{aligned} y_\alpha(t) &= \frac{c_0}{N} + \frac{1}{N} \sum_{j=1}^{N-1} c_j e^{\frac{2\pi j \alpha i}{N}} e^{(\lambda_j - 1)t} \\ &= \frac{c_0}{N} + \frac{1}{N} \sum_{j=1}^{N-1} c_j e^{\frac{2\pi j \alpha i}{N}} e^{(-1 + \sum_{l=0}^{N-1} [(\cos \frac{2\pi jl}{N} + i \sin \frac{2\pi jl}{N}) x_l])t} \\ &= \frac{c_0}{N} + \frac{1}{N} \sum_{j=1}^{N-1} c_j e^{(-1 + \sum_{l=0}^{N-1} x_l \cos(\frac{2\pi jl}{N}))t} e^{i[2\pi j \frac{\alpha}{N} + \sum_{l=0}^{N-1} x_l t \sin(\frac{2\pi jl}{N})]} \end{aligned} \quad (4.64)$$

Considering just the real part and defining the relaxation times as

$$\tau_j = \frac{1}{1 - \sum_{l=0}^{N-1} x_l \cos\left(\frac{2\pi jl}{N}\right)} \quad j = 1, \dots, N-1 \quad (4.65)$$

the final result is

$$y_\alpha(t) = \frac{c_0}{N} + \frac{1}{N} \sum_{j=1}^{N-1} c_j e^{-\frac{t}{\tau_j}} \cos\left[2\pi j \frac{\alpha}{N} + \sum_{l=0}^{N-1} x_l \sin\left(\frac{2\pi jl}{N}\right) t\right] \quad (4.66)$$

where the coefficients c_j are given by the initial conditions on the probes.

Considering for example again the case in which $y_0(0) = \kappa$ and all the other $y_j(0) = 0$ with $j \neq 0$, where $\kappa = 10$ and $N = 10$, the trends of the perturbations are represented in figure 4.16.

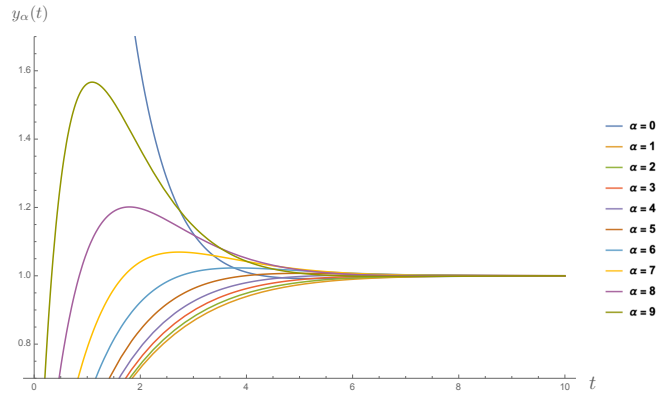


Figure 4.16: System of 10 probes with all the *elastic constants*

Instead, considering just m_1 , the perturbations' trends of the equivalent system are those in figure 4.17.

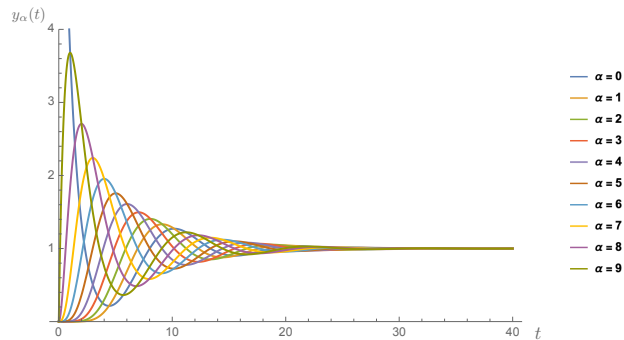


Figure 4.17: System of 10 probes with only m_1

The probes seem to relax faster towards the crystal configuration when we consider all the *elastic constants*.

This faster relaxation comes from the fact that the relaxation times τ_j are smaller.

Considering the definition (4.65) of the relaxation time and splitting from the summation the terms with $l = 1$ and $l = 0$, (4.65) becomes

$$\tau_j = \frac{1}{1 - \cos\left(\frac{2\pi j}{N}\right) + \sum_{m=2}^{N-1} \frac{m_m}{m_1} - \sum_{l=2}^{N-1} \frac{m_l}{m_1} \cos\left(\frac{2\pi jl}{N}\right)} \quad j = 1, \dots, N-1 \quad (4.67)$$

For $m_\gamma = m_1 \delta_{\gamma 1}$ we just have

$$\tau_j = \frac{1}{1 - \cos\left(\frac{2\pi j}{N}\right)} \quad (4.68)$$

and the more are the m_γ considered the more are the terms added in the denominator.

In particular the sum of the added terms is always ≥ 0 . Indeed

$$\sum_{m=2}^{N-1} \frac{m_m}{m_1} - \sum_{l=2}^{N-1} \frac{m_l}{m_1} \cos\left(\frac{2\pi jl}{N}\right) \geq 0 \quad (4.69)$$

since $\cos\left(\frac{2\pi jl}{N}\right) \leq 1$.

That means that every time a new m_γ is added, the denominator increases, τ_j decreases and the relaxation towards the asymptotic $y_\alpha^* = \frac{\kappa}{N}$ becomes faster.

The fact that the more are the *elastic constants* the faster is the relaxation allows to state that, if the crystal pattern is detected in the case of one single *elastic constant* (as it was done in the previous analysis), surely the crystal configuration will be reached also in the not approximated case with all the *elastic constants*.

Chapter 5

Thermal stability

Once the relaxation towards the crystal configuration and its mechanical stability have been studied, it is crucial also to analyse the thermal stability of the system.

In order to estimate the role of thermal fluctuations, thermal noise can be added to (4.26), getting

$$\dot{y}_\alpha = y_{\alpha+1} - y_\alpha + \sqrt{2T} \xi_\alpha, \quad \alpha = 0, \dots, N-1 \quad (5.1)$$

where the ξ_α are standard white noise processes, and T is the noise-strength, e.g. from a thermal reservoir at temperature T . The Smoluchowski equation that comes from eq. (5.1) is

$$\frac{\partial \rho_t}{\partial t}(y) = \sum_{\alpha=0}^{N-1} \frac{\partial}{\partial y_\alpha} [(y_\alpha - y_{\alpha+1}) \rho_t(y)] + T \frac{\partial^2 \rho_t}{\partial y_\alpha^2}(y) \quad (5.2)$$

for the density $\rho_t(y) = \rho_t(y_0, \dots, y_{N-1})$ on $(S^1)^N$.

The stationary density for eq. (5.2) is

$$\rho_{\text{stat}}(y) = \frac{1}{Z} e^{-\frac{V(y)}{T}} \quad \text{with } V(y) = \frac{1}{4} \sum_{\alpha=0}^{N-1} (y_{\alpha+1} - y_\alpha)^2 \quad (5.3)$$

This can be proven. Indeed from (5.3)

$$\frac{\partial \rho_{\text{stat}}}{\partial y_\alpha}(y) = -\frac{1}{T} \rho_{\text{stat}}(y) (y_\alpha - \frac{1}{2}[y_{\alpha-1} + y_{\alpha+1}]) \quad (5.4)$$

considering that each y_α appears in two terms of the summation $\sum_\alpha (y_{\alpha+1} - y_\alpha)^2$.

Hence

$$\begin{aligned} [(y_\alpha - y_{\alpha+1}) \rho_{\text{stat}}(y)] + T \frac{\partial \rho_{\text{stat}}}{\partial y_\alpha}(y) &= (y_\alpha - y_{\alpha+1}) \rho_{\text{stat}}(y) - \rho_{\text{stat}}(y) (y_\alpha - \frac{1}{2}[y_{\alpha-1} + y_{\alpha+1}]) \\ &= \frac{1}{2} \rho_{\text{stat}}(y_{\alpha-1} - y_{\alpha+1}) \end{aligned} \quad (5.5)$$

and

$$\begin{aligned} \frac{\partial}{\partial y_\alpha} [\rho_{\text{stat}}(y) (y_{\alpha-1} - y_{\alpha+1})] &= \frac{\partial \rho_{\text{stat}}(y)}{\partial y_\alpha} (y_{\alpha-1} - y_{\alpha+1}) \\ &= -\frac{1}{T} \rho_{\text{stat}}(y) \left(y_\alpha - \frac{1}{2} [y_{\alpha-1} + y_{\alpha+1}] \right) (y_{\alpha-1} - y_{\alpha+1}) \end{aligned} \quad (5.6)$$

Following the right-hand side of equation (5.2) and summing over α all the contributions of equation (5.6), the result is zero.

However, there is no detailed balance in the sense that the current components $(y_\alpha - y_{\alpha+1}) \rho_{\text{stat}}(y) + T \frac{\partial \rho_{\text{stat}}(y)}{\partial y_\alpha} \neq 0$ do not vanish identically.

The analysis done in this chapter until now is correct, but it starts from an approximate dynamics' equation that is eq. (5.1). It seems more complete to analyse the role of thermal fluctuations for the exact noisy equation

$$\Gamma \dot{y}_\alpha = \sum_\gamma M_{\alpha\gamma} y_\gamma + \left(\frac{2\Gamma}{\beta} \right)^{1/2} \xi_\alpha \quad (5.7)$$

The related Smoluchowski equation is

$$\begin{aligned} \frac{\partial \rho_t}{\partial t}(y) &= \sum_{\alpha=0}^{N-1} -\frac{\partial}{\partial y_\alpha} \left[\sum_\gamma M_{\alpha\gamma} y_\gamma \rho_t(y) \right] + T \frac{\partial^2 \rho_t(y)}{\partial y_\alpha^2}(y) \\ &= \sum_{\alpha=0}^{N-1} -\frac{\partial}{\partial y_\alpha} \left[\sum_{\gamma=1}^{N-1} m_\gamma (y_{\alpha+\gamma} - y_\alpha) \rho_t(y) \right] + T \frac{\partial^2 \rho_t(y)}{\partial y_\alpha^2}(y) \end{aligned} \quad (5.8)$$

The stationary distribution coincides with the Boltzmann distribution

$$\rho_{\text{stat}}(y) = \frac{1}{Z} e^{-\beta V(y)} \quad (5.9)$$

for the effective potential

$$V(y) = \frac{1}{4} \sum_{\gamma>0} m_\gamma \sum_{\alpha} (y_{\alpha+\gamma} - y_\alpha)^2 \quad (5.10)$$

Indeed it is possible to use the same reasoning of equation (5.3), writing that

$$\frac{\partial \rho_{\text{stat}}(y)}{\partial y_\alpha}(y) = -\frac{1}{T} \rho_{\text{stat}}(y) \sum_{\gamma>0} m_\gamma \left[y_\alpha - \frac{1}{2} (y_{\alpha-\gamma} + y_{\alpha+\gamma}) \right], \quad (5.11)$$

from which

$$-\sum_{\gamma=1}^{N-1} m_\gamma (y_{\alpha+\gamma} - y_\alpha) \rho_{\text{stat}}(y) + T \frac{\partial \rho_{\text{stat}}(y)}{\partial y_\alpha}(y) = \frac{1}{2} \sum_{\gamma=1}^{N-1} m_\gamma \rho_{\text{stat}}(y) [y_{\alpha-\gamma} - y_{\alpha+\gamma}] \quad (5.12)$$

and equation (5.8) becomes

$$\begin{aligned} \frac{\partial \rho_{\text{stat}}(y)}{\partial t}(y) &= \sum_{\alpha} \frac{\partial}{\partial y_{\alpha}} \left[\frac{1}{2} \sum_{\gamma=1}^{N-1} m_{\gamma} \rho_{\text{stat}}(y) [y_{\alpha-\gamma} - y_{\alpha+\gamma}] \right] \\ &= \sum_{\alpha} \sum_{\gamma=1}^{N-1} \frac{m_{\gamma}}{2} [y_{\alpha-\gamma} - y_{\alpha+\gamma}] \frac{\partial \rho_{\text{stat}}(y)}{\partial y_{\alpha}}(y) \end{aligned} \quad (5.13)$$

Therefore, in order to prove that (5.9) is really stationary, the condition that should be satisfied is

$$\sum_{\alpha} \sum_{\gamma=1}^{N-1} \left[m_{\gamma} (y_{\alpha-\gamma} - y_{\alpha+\gamma}) \sum_{\delta>0} m_{\delta} (y_{\alpha} - \frac{1}{2}(y_{\alpha-\delta} + y_{\alpha+\delta})) \right] = 0 \quad (5.14)$$

Let us consider the terms inside the summation over α . There are two types of terms, those with $\delta = \gamma$ and those with $\delta \neq \gamma$.

In the first case, without considering the constants m_{γ} and m_{δ} , the shape of the terms is

$$y_{\alpha-\gamma} y_{\alpha} - y_{\alpha+\gamma} y_{\alpha} - \frac{1}{2} (y_{\alpha-\gamma}^2 - y_{\alpha+\gamma}^2)$$

and summing over α each of these terms gives 0.

For $\delta \neq \gamma$ the terms inside the summation over α are

$$y_{\alpha-\gamma} y_{\alpha} - y_{\alpha} y_{\alpha+\gamma} - \frac{1}{2} (y_{\alpha-\gamma} y_{\alpha-\delta} + y_{\alpha-\gamma} y_{\alpha+\delta} - y_{\alpha+\gamma} y_{\alpha-\delta} - y_{\alpha+\gamma} y_{\alpha+\delta})$$

and also in this case summing over α each term gives 0.

Therefore it has been proved that the stationary distribution is

$$\rho_{\text{stat}}(y) = \frac{1}{Z} \exp \left[-\frac{\beta}{4} \sum_{\gamma>0} m_{\gamma} \sum_{\alpha} (y_{\alpha+\gamma} - y_{\alpha})^2 \right] \quad (5.15)$$

In particular this is a multivariate normal distribution (see [7]) of the form

$$f(\mathbf{x}) = \frac{1}{Z} \exp \left[-\frac{1}{2} (\mathbf{x} - \mu)^T \Sigma^{-1} (\mathbf{x} - \mu) \right] \quad (5.16)$$

for which μ is the mean and Σ is the variance (σ^2).

For eq. (5.15)

$$\mu = 0 \quad \text{and} \quad \Sigma = \frac{1}{\beta}$$

and so

$$\frac{1}{\beta} = \sigma^2 = \frac{1}{2} \sum_{\gamma} m_{\gamma} \langle (y_{\alpha+\gamma} - y_{\alpha})^2 \rangle - \mu^2 = \frac{1}{2} \sum_{\gamma} m_{\gamma} \langle (y_{\alpha+\gamma} - y_{\alpha})^2 \rangle \quad (5.17)$$

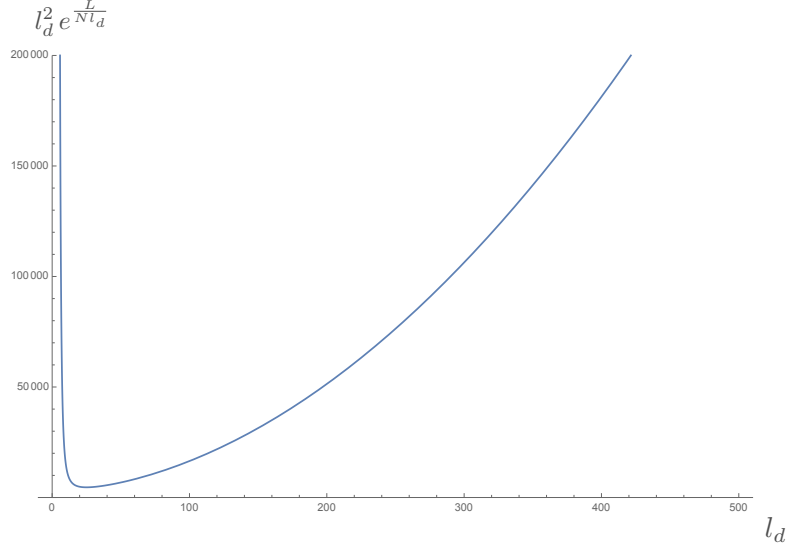


Figure 5.1: Representation of the $\langle (y_{\alpha+1} - y_\alpha)^2 \rangle$ behaviour

Assuming now for simplicity that m_γ is negligible for $\gamma \geq 2$,

$$\langle (y_{\alpha+1} - y_\alpha)^2 \rangle \simeq \frac{2}{\beta m_1} \quad (5.18)$$

In the globally strong non-equilibrium regime

$$\langle (y_{\alpha+1} - y_\alpha)^2 \rangle \simeq \frac{2l_d^2}{\beta \zeta j^* B} e^{\frac{L}{N l_d}} \quad (5.19)$$

For $\frac{L}{N} \gg l_d$ the thermal fluctuations exponentially blow up (due to the factor $e^{\frac{L}{N l_d}}$). If instead $l_d \gg \frac{L}{N}$ there is again a blowing up due to the l_d^2 -dependence.

This behaviour can be briefly seen in figure 5.1, where the function

$$f(l_d, \frac{L}{N}) = l_d^2 e^{\frac{L}{N l_d}} \quad (5.20)$$

has been plotted in dependence of l_d fixing a random value $\frac{L}{N} = 50$. It is easy to notice that only for values $l_d \approx \frac{L}{N}$ the function (that represents $\langle (y_{\alpha+1} - y_\alpha)^2 \rangle$) does not blow up. In particular the minimum of the function is easy to get, just differentiating, and it is $l_d = \frac{1}{2} \frac{L}{N}$.

Thus the nearly optimal regime for which thermal fluctuations do not destroy the crystal pattern is $\frac{L}{N} \approx l_d$.

Going back to formula 5.19, in the nearly optimal regime $\frac{L}{N} \approx l_d$, the condition of thermal stability $\langle (y_{\alpha+1} - y_\alpha)^2 \rangle \ll (L/N)^2$ yields the inequality

$$j^* \gg \frac{1}{\beta \zeta B} \quad (5.21)$$

This provides a lower bound on the colloidal current in order to generate a crystal pattern that is stable against thermal fluctuations.

Chapter 6

Thermodynamic limit

The goal of this chapter is to analyse how the system behaves in the thermodynamic limit.

The thermodynamic limit of a system is the limit for a large number N of particles where the volume is taken to grow in proportion with the number of particles.

For the configuration analysed in this thesis, the thermodynamic limit is defined as the limit of a system with a large ring length, with the probe density held fixed:

$$N \rightarrow \infty, \quad L \rightarrow \infty, \quad \frac{N}{L} = \text{constant} \quad (6.1)$$

The idea is to see if the forces, the currents and all the other quantities that characterize the finite system are consistent also with the thermodynamic limit or instead, in such a limit, show some problems, divergences.

First of all let us notice that both the *globally strong driving regime* hypothesis and the *probes' isolation* condition are consistent with the thermodynamic limit.

Indeed, for $L \rightarrow \infty$ it is clear that $L \gg l_d$ and again it is possible to fix the probes density to a value smaller than $\frac{1}{2\delta}$ such that their isolation condition can be maintained.

Let us now focus on the expression of the probes' induced non reactive forces.

The equation derived for such forces in the globally strong driving regime for a finite number N of probes in a ring of a finite length L was

$$f_\alpha(x) = f^{\text{drift}}(x) + f_\alpha^{\text{int}}(x) = \zeta j_x A - \frac{\zeta j_x B}{l_d} \sum_{\gamma \neq \alpha} e^{-\frac{(x_\gamma - x_\alpha)^o}{l_d}} \quad (6.2)$$

Does this form of the forces present any problem in the thermodynamic limit?

The possible issues are the convergence of the infinite series and the dependence on N and L of all the terms.

Let us start from the convergence of the series

$$\sum_{\gamma \neq \alpha} e^{-\frac{(x_\gamma - x_\alpha)^o}{l_d}} \quad (6.3)$$

for an infinite number of possible γ that index the probes. In order to do that the comparison test for the series' convergence will be used.

Such a test states that, if we have a series

$$\sum_{\gamma=1}^{\infty} a_\gamma \quad (6.4)$$

that converges and $b_\gamma \leq a_\gamma$ for every γ , then also the series

$$\sum_{\gamma=1}^{\infty} b_\gamma \quad (6.5)$$

converges.

Let us then take the series

$$\sum_{\gamma=1}^{\infty} e^{-\frac{\gamma\delta}{l_d}} \quad (6.6)$$

where δ is the range of the probe-colloids interaction. As $e^{-\frac{\delta}{l_d}} < 1$, this is a geometric series that converges.

Because of the probes' isolation condition we know that $(x_\gamma - x_\alpha)^o \geq 2\delta$ and so that $e^{-\frac{(x_\gamma - x_\alpha)^o}{l_d}} < e^{-\frac{\gamma\delta}{l_d}}$.

Then, by comparison test, also

$$\sum_{\gamma \neq \alpha} e^{-\frac{(x_\gamma - x_\alpha)^o}{l_d}} \quad (6.7)$$

converges.

In equation (6.2) ζ , l_d , A and B do not depend on N and L . The colloidal current j_x instead was defined in eq. (2.26) as

$$j_x = \frac{\rho^0 \varepsilon}{\zeta Z(x)} \quad (6.8)$$

where, in the globally strong driving regime,

$$Z(x) = 1 + \frac{NA}{L} - \frac{\beta\varepsilon}{L} B \sum_{\alpha, \gamma \neq \alpha} e^{-\beta\varepsilon(x_\gamma - x_\alpha)^o} \quad (6.9)$$

In equation (6.9), for the thermodynamic limit, the double summation behaviour should be analysed.

The sum over α is of order N , therefore

$$\sum_{\alpha, \gamma \neq \alpha} e^{-\beta \varepsilon (x_\gamma - x_\alpha)^\circ} \sim N \sum_{\gamma \neq \alpha} e^{-\frac{(x_\gamma - x_\alpha)^\circ}{l_d}} \quad (6.10)$$

and from the previous reasoning the sum over $\gamma \neq \alpha$ converges.

In the end, in the thermodynamic limit, the form of $Z(x)$ is

$$Z(x) \simeq 1 + \frac{NA}{L} - \frac{N\beta\varepsilon}{L} B \sum_{\gamma \neq \alpha} e^{-\beta \varepsilon (x_\gamma - x_\alpha)^\circ}, \quad (6.11)$$

that is well defined with $N \rightarrow \infty$ and $L \rightarrow \infty$ keeping $\frac{N}{L}$ constant.

Considering now the linearized dynamics near the crystal configuration, governed by

$$\Gamma \dot{y}_\alpha = \sum_{\gamma} M_{\alpha\gamma} y_\gamma = \sum_{\gamma=1}^{N-1} m_\gamma (y_{\alpha+\gamma} - y_\alpha), \quad (6.12)$$

m_γ is defined as

$$m_\gamma = \frac{\zeta j_x^* B}{l_d^2 (1 - e^{-\frac{L}{N l_d}})} e^{-\frac{L}{N l_d} \alpha} \quad (6.13)$$

where j_x^* is just the colloidal current in the case of the equidistant probes configuration. So also the *elastic constants* m_γ are well defined in the thermodynamic limit.

Let us remind also that, for the perturbations' dynamics, it was used the very simplified differential equation

$$\dot{y}_\alpha = y_{\alpha+1} - y_\alpha \quad (6.14)$$

for which all the constants m_γ except m_1 were considered negligible and time was rescaled by $\frac{\Gamma}{m_1}$.

Also in the case of the thermodynamic limit such a simplification can be used as, with the growing of α , there is still a strong exponential decay of m_α .

So far, everything that was computed for the case of a finite system seems to be in agreement with the thermodynamic limit.

However, for such a limit, we still have to analyse the possibility of a relaxation to a crystal pattern.

Equation (4.65) gives an expression for the relaxation time of a finite probes' system and in particular shows the dependence of τ_{relax} on N^2 (where N is the number of probes).

τ_{relax} was defined as the characteristic time in which the Poisson wave that describes the propagation of the perturbation *spreads* over the whole ring.

It is clear that the dependence on N^2 makes impossible the relaxation in a finite time for the thermodynamic limit.

The same argument can be used to state also the presence of a non finite *echo time* ($\propto N$) in the thermodynamic limit.

For a finite system, the wave representing the perturbation's propagation travels several laps of the ring and passes several times by each probe, before definitely relaxing to the crystal pattern. For an infinite system this is not possible. As time passes, the *wave* reaches more and more probes but will never pass by them more than once.

At the end in the limit $N \rightarrow \infty$ a global relaxation to the crystal pattern in a finite time will never be reached.

The analysis, in the thermodynamic limit, will then be different and focused on the local behaviour of the probes and on how they respond to a time-dependent perturbation.

The idea is to assume that at time 0 the infinite system has a crystal configuration such that, for each probe α , $y_\alpha(0) = 0$.

Now a finite portion of the ring is selected (see figure 6.1). The number of probes in that portion is n and they are indexed by $0, \dots, n-1$.

The probe that comes immediately after (in the direction of the driving force ε) will then have index n .

The goal of this chapter is to study the stability of such a configuration by considering a time-dependent perturbation on the n -th probe. This perturbation represents in a simple way a possible thermal oscillation of the crystal or any other behaviour that could break, at least for some time, the crystal pattern.

In particular the perturbation on the n -th probe contains, hypothetically, the contribution of all the other infinite probes (the *bath*).

How does this perturbation propagate inside the finite portion of probes? Does the perturbation propagate differently to probe 0 and to probe $n-1$? Does it depend on its frequency?

The system of probes obeys the linear dynamics already discussed. In particular, considering $m_\gamma = m_1 \delta_{\gamma 1}$ and rescaling the time the dynamics will be of the form

$$\dot{y}_\alpha = y_{\alpha+1} - y_\alpha \quad (6.15)$$

Let us start by considering a periodic time-dependent perturbation on the n -th probe

$$y_n(t) = B \cos(\omega t) \quad (6.16)$$

In this way

$$\dot{y}_{n-1} = B \cos(\omega t) - y_{n-1}, \quad \dot{y}_{n-2} = y_{n-1} - y_{n-2} \quad \text{and so on} \quad (6.17)$$

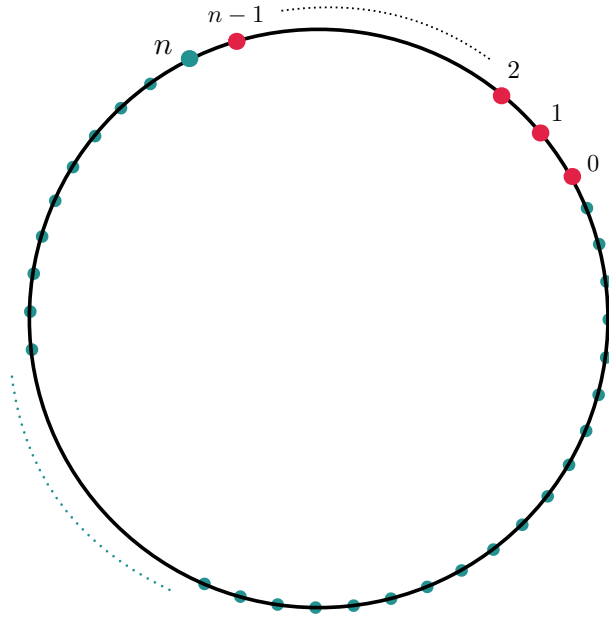


Figure 6.1: Portion of n red probes in the thermodynamic limit. The perturbation given by the infinite light blue *bath* is modeled as a time dependent perturbation for the probe n .

Just through iteration it is possible to find how y_{n-1} , y_{n-2} , y_{n-3}, \dots evolve. For example, the explicit expression for y_{n-1} , with initial condition $y_{n-1}(0) = 0$, is

$$y_{n-1} = \frac{B}{1 + \omega^2} [\cos(\omega t) + \omega \sin(\omega t) - e^{-t}] \quad (6.18)$$

And just by iteration we can get expressions for all the perturbations of the probes inside the segment, given their initial values.

Below, some trends of the perturbations for different values of ω are presented (fixing $B=1$).

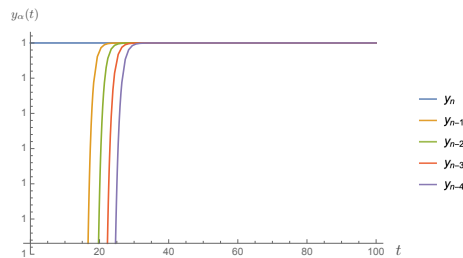
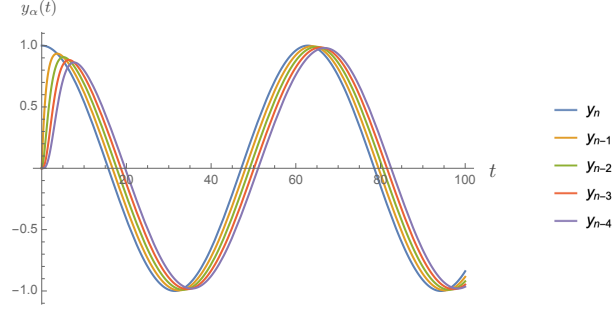
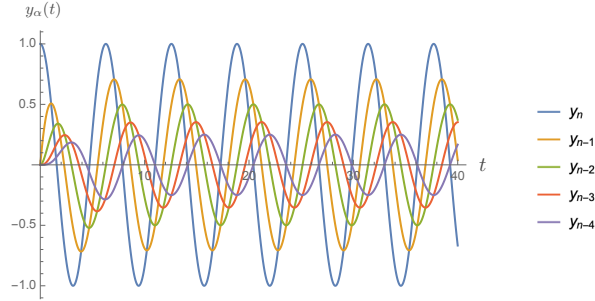


Figure 6.2: $\omega = 0$

Figure 6.3: $\omega = 0.1$ Figure 6.4: $\omega = 1$

It is clear that the perturbation on the probe n propagates inside the portion with an amplitude that decreases with the distance from the probe n . The decreasing depends also on the frequency of the signal. The bigger is the frequency, the smaller are the probes' oscillations due to the initial perturbation.

What if the time-dependent perturbation on the n -th probe is given by the sum of two (or more) sinusoidal oscillations with different frequency?

In order to study this a different approach will be used. The perturbation on the n -th probe is written as

$$y_n(t) = B_1 e^{i\omega_1 t} + B_2 e^{i\omega_2 t} \quad (6.19)$$

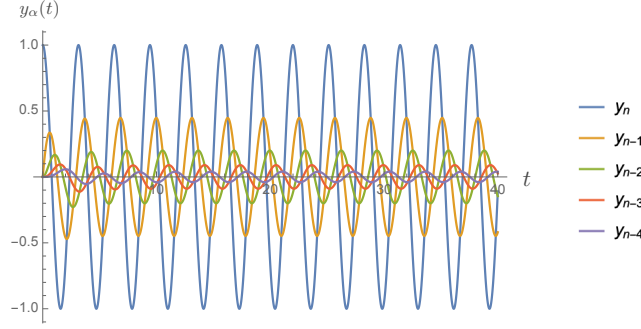
where the oscillation is a wave written as a sum of two complex exponentials (with different frequencies ω_1 and ω_2). If we want the initial perturbation to be the sum of two cosines, at the end just the real part will be considered.

In order to solve eq. (6.15), we consider the ansatz

$$y_\alpha(t) = C_{1_\alpha} e^{i\nu_1 t} + C_{2_\alpha} e^{i\nu_2 t} \quad (6.20)$$

Inserting (6.20), equation (6.15) becomes

$$(i\nu_1 + 1)C_{1_\alpha} e^{i\nu_1 t} + (i\nu_2 + 1)C_{2_\alpha} e^{i\nu_2 t} = C_{1_{\alpha+1}} e^{i\nu_1 t} + C_{2_{\alpha+1}} e^{i\nu_2 t} \quad (6.21)$$

Figure 6.5: $\omega = 2$

From which

$$C_{1_\alpha} = C_{1_{\alpha+1}}(i\nu_1 + 1)^{-1} \quad \text{and} \quad C_{2_\alpha} = C_{2_{\alpha+1}}(i\nu_2 + 1)^{-1} \quad (6.22)$$

In general $(i\nu + 1)^{-1}$ can be rewritten in exponential form as

$$(i\nu + 1)^{-1} = (\nu^2 + 1)^{-\frac{1}{2}} e^{-i \arctan(\nu)} \quad (6.23)$$

and so

$$C_{1_\alpha} = C_{1_{\alpha+1}}(\nu_1^2 + 1)^{-\frac{1}{2}} e^{-i \arctan(\nu_1)} \quad (6.24)$$

$$C_{2_\alpha} = C_{2_{\alpha+1}}(\nu_2^2 + 1)^{-\frac{1}{2}} e^{-i \arctan(\nu_2)} \quad (6.25)$$

In 6.20, in order to be more rigorous, a dependence on α of the two frequencies ν_1 and ν_2 should have been written. But the iterative differential equation does not change the frequencies and so ν_1 and ν_2 do not have to depend on α .

In particular, because of 6.19, $\nu_1 = \omega_1$ and $\nu_2 = \omega_2$ for every α of the *portion*.

At the end

$$y_{n-k}(t) = \frac{B_1}{(\omega_1^2 + 1)^{\frac{k}{2}}} e^{i(\omega_1 t - k \arctan(\omega_1))} + \frac{B_2}{(\omega_2^2 + 1)^{\frac{k}{2}}} e^{i(\omega_2 t - k \arctan(\omega_2))} \quad (6.26)$$

and taking just the real part

$$y_{n-k}(t) = \frac{B_1}{(\omega_1^2 + 1)^{\frac{k}{2}}} \cos[\omega_1 t - k \arctan(\omega_1)] + \frac{B_2}{(\omega_2^2 + 1)^{\frac{k}{2}}} \cos[\omega_2 t - k \arctan(\omega_2)] \quad (6.27)$$

The same reasoning can be used also for a single sinusoidal perturbation

$$y_n(t) = B e^{i\omega t} \quad (6.28)$$

and at the end, taking just the real part, the perturbation propagates as

$$y_{n-k}(t) = \frac{B}{(\omega^2 + 1)^{\frac{k}{2}}} \cos[\omega t - k \arctan(\omega)] \quad (6.29)$$

It is clear that the propagation of a signal from the n -th probe is linear and so that a sum of oscillations can just be analysed by considering each signal individually.

6.1 White noise on probe n

Let us now consider a white noise $\xi(t)$ on the n -th probe and see how it influences the crystal configuration of the probes. The studies of the effect of noise are very important and sometimes white noise can also play a surprising ordering role in the system (see for example [6]).

In order to analyse the behaviour of the system Fourier transforms will be used this time.

Defining $\mathcal{F}[y_\alpha(t)] \equiv \hat{Y}_\alpha(\omega)$ and Fourier transforming all the terms, equation (6.15) becomes

$$i\omega \hat{Y}_\alpha(\omega) + \hat{Y}_\alpha(\omega) = \hat{Y}_{\alpha+1}(\omega) \quad (6.30)$$

from which

$$\hat{Y}_\alpha(\omega) = \frac{\hat{Y}_{\alpha+1}(\omega)}{1 + i\omega} \quad (6.31)$$

Iterating this process,

$$\hat{Y}_\alpha(\omega) = \left(\frac{1}{1 + i\omega} \right)^{n-\alpha} \hat{Y}_n(\omega) \quad (6.32)$$

White noise $\xi(t)$ is defined such that

$$\langle \xi(t) \rangle = 0 \quad \langle \xi(t) \xi(t') \rangle = \delta(t - t') \quad (6.33)$$

and defining $\hat{\xi}(\omega)$ as the *Fourier transform* of $\xi(t)$ it is clear that

$$\langle \hat{\xi}(\omega) \hat{\xi}(\nu) \rangle = \delta(\omega + \nu). \quad (6.34)$$

From eq. (6.32) and the definition of Fourier transforms, we get

$$y_\alpha(t) = \int d\omega e^{i\omega t} \hat{\xi}(\omega) \left(\frac{1}{1 + i\omega} \right)^{n-\alpha} \quad (6.35)$$

and from this it is possible to compute the correlation function $\langle y_\alpha(t) y_\beta(s) \rangle$.

$$\langle y_\alpha(t) y_\beta(s) \rangle = \int d\omega \int d\nu e^{i\omega t} e^{i\nu s} \langle \hat{\xi}(\omega) \hat{\xi}(\nu) \rangle \left(\frac{1}{1 + i\omega} \right)^{n-\alpha} \left(\frac{1}{1 + i\nu} \right)^{n-\beta} \quad (6.36)$$

And considering (6.34)

$$\langle y_\alpha(t)y_\beta(s) \rangle = \int d\omega e^{i\omega(t-s)} \left(\frac{1}{1+\omega^2} \right)^{n-\beta} \left(\frac{1}{1+i\omega} \right)^{\beta-\alpha}. \quad (6.37)$$

Rewriting

$$\left(\frac{1}{1+i\omega} \right)^{\beta-\alpha} = \left(\frac{1}{1+\omega^2} \right)^{\frac{\beta-\alpha}{2}} e^{i(\alpha-\beta) \arctan \omega} \quad (6.38)$$

eq. (6.37) becomes

$$\langle y_\alpha(t)y_\beta(s) \rangle = \int d\omega e^{i[\omega(t-s)+(\alpha-\beta) \arctan \omega]} \left(\frac{1}{1+\omega^2} \right)^{\frac{2n-\alpha-\beta}{2}} \quad (6.39)$$

The imaginary part is

$$\text{Im} \langle y_\alpha(t)y_\beta(s) \rangle = i \int d\omega \sin[\omega(t-s) + (\alpha-\beta) \arctan \omega] \left(\frac{1}{1+\omega^2} \right)^{\frac{2n-\alpha-\beta}{2}} \quad (6.40)$$

and it is 0 as we are integrating an odd function in a symmetric domain.

The real part is instead

$$\text{Re} \langle y_\alpha(t)y_\beta(s) \rangle = \int d\omega \cos[\omega(t-s) + (\alpha-\beta) \arctan \omega] \left(\frac{1}{1+\omega^2} \right)^{\frac{2n-\alpha-\beta}{2}} \quad (6.41)$$

In particular

$$\langle y_\alpha(t)^2 \rangle = \int d\omega \left(\frac{1}{1+\omega^2} \right)^{n-\alpha} \quad (6.42)$$

that does not depend on time t .

It is possible to plot for example $\langle y_0(t)^2 \rangle$ (see figure 6.6) varying the number n of the probes of the *section*, that means increasing the distance of probe 0 from the perturbation at probe n .

It is clear that the bigger is the distance the smaller is the influence of white noise on a probe.

Another quantity that is interesting to plot is $\langle (y_\alpha(t) - y_\beta(t))^2 \rangle$, always varying n .

$$\begin{aligned} \langle (y_\alpha(t) - y_\beta(t))^2 \rangle &= \int d\omega \int d\nu e^{i\omega t} e^{i\nu t} \langle \hat{\xi}(\omega) \hat{\xi}(\nu) \rangle \left(\left(\frac{1}{1+i\omega} \right)^{n-\alpha} - \left(\frac{1}{1+i\omega} \right)^{n-\beta} \right) \times \\ &\times \left(\left(\frac{1}{1+i\nu} \right)^{n-\alpha} - \left(\frac{1}{1+i\nu} \right)^{n-\beta} \right) = \quad (6.43) \\ &= \int d\omega \left(\left(\frac{1}{1+i\omega} \right)^{n-\alpha} - \left(\frac{1}{1+i\omega} \right)^{n-\beta} \right) \times \left(\left(\frac{1}{1-i\omega} \right)^{n-\alpha} - \left(\frac{1}{1-i\omega} \right)^{n-\beta} \right) \end{aligned}$$

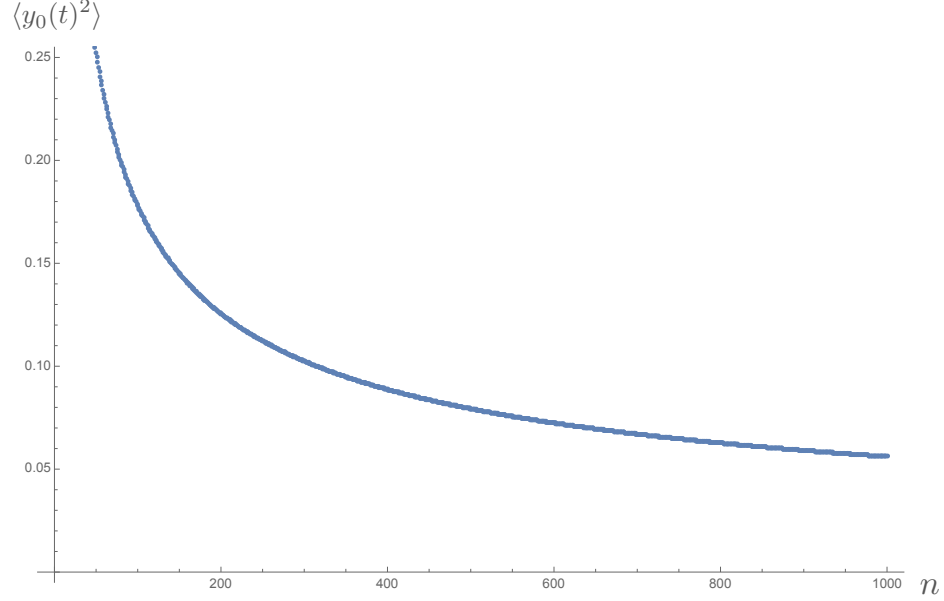


Figure 6.6: Plot of $\langle y_0(t)^2 \rangle$ vs n given $y_n(t) = \xi(t)$.

The multiplication of the two brackets gives

$$\begin{aligned} & \left(\frac{1}{1+\omega^2} \right)^{n-\alpha} + \left(\frac{1}{1+\omega^2} \right)^{n-\beta} - \left(\frac{1}{1+i\omega} \right)^{n-\alpha} \left(\frac{1}{1-i\omega} \right)^{n-\beta} - \left(\frac{1}{1+i\omega} \right)^{n-\beta} \left(\frac{1}{1-i\omega} \right)^{n-\alpha} = \\ = & \left(\frac{1}{1+\omega^2} \right)^{n-\alpha} + \left(\frac{1}{1+\omega^2} \right)^{n-\beta} - \left(\frac{1}{1+\omega^2} \right)^{n-\beta} \left(\frac{1}{1+i\omega} \right)^{\beta-\alpha} - \left(\frac{1}{1+\omega^2} \right)^{n-\beta} \left(\frac{1}{1-i\omega} \right)^{\beta-\alpha} \end{aligned}$$

Observing that

$$\frac{1}{1+i\omega} = \frac{1}{\sqrt{1+\omega^2}} e^{-i \arctan \omega} \quad \frac{1}{1-i\omega} = \frac{1}{\sqrt{1+\omega^2}} e^{i \arctan \omega} \quad (6.44)$$

and substituting, at the end

$$\begin{aligned} \langle (y_\alpha(t) - y_\beta(t))^2 \rangle = \int d\omega \{ & \left(\frac{1}{1+\omega^2} \right)^{n-\alpha} + \left(\frac{1}{1+\omega^2} \right)^{n-\beta} - 2 \left(\frac{1}{1+\omega^2} \right)^{\frac{2n-\alpha-\beta}{2}} \times \\ & \times \cos[(\beta - \alpha) \arctan \omega] \} \quad (6.45) \end{aligned}$$

This formula can be plotted for example fixing $\alpha = 0$ and $\beta = 1$ and varying the number n of probes and what we get is figure 6.7.

In particular figures 6.6 and 6.7 show how the *noisy* perturbation to the crystal configuration does not influence a lot distant probes. In particular both $\langle y_\alpha(t)^2 \rangle$ and $\langle (y_\alpha(t) - y_{\alpha+1}(t))^2 \rangle$ decrease exponentially in distance from probe n .

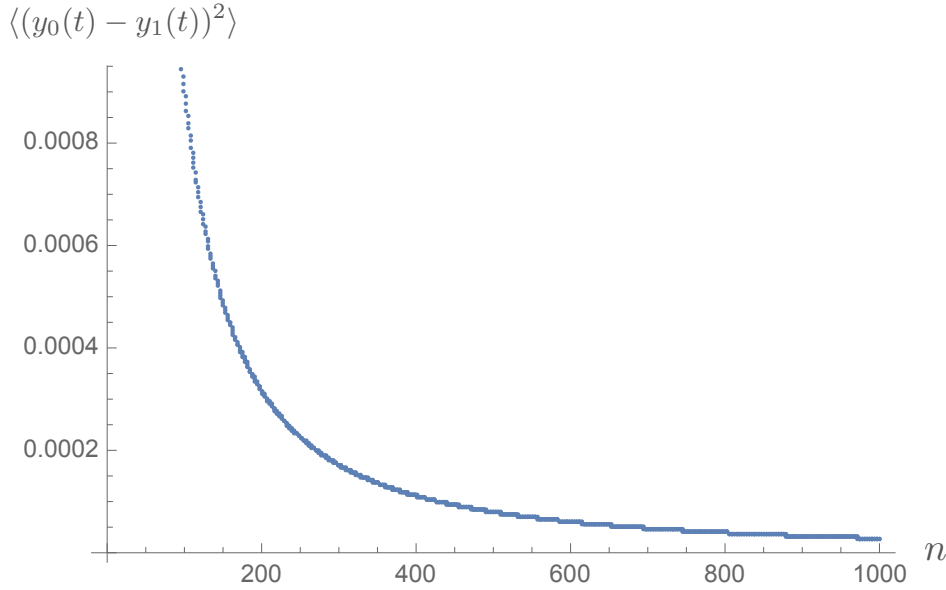


Figure 6.7: Plot of $\langle (y_0(t) - y_1(t))^2 \rangle$ vs n given $y_n(t) = \xi(t)$.

6.2 The damping law

So far, in this chapter, different methods were used in order to study the behaviour of an arbitrarily large system of probes in which the crystal configuration is broken by a time dependent perturbation.

We now want to clarify the analysis done until now. Among the different methods that were used we would like to identify the best one in order to get a clear law on how a perturbation propagates in such a system, depending on frequency and distance.

This time the perturbing signal considered is a sine function like

$$y_n(t) = k \sin(\nu t). \quad (6.46)$$

This is due to the fact that this signal (differently from the cosine) starts from 0 at time 0. This is physically meaningful for a system that is in a crystal configuration and starts to feel for the first time a perturbation at time zero.

Let us consider equation (6.15) for $\alpha = n - 1$, that is

$$\dot{y}_{n-1} = y_n - y_{n-1} \quad (6.47)$$

The first method used to solve this equation is the standard formula for first order differential equations and the result is

$$y_{n-1}(t) = -\frac{ke^{-t}(-\nu + e^t \nu \cos(\nu t) - e^t \sin(\nu t))}{1 + \nu^2} \quad (6.48)$$

where the initial condition is $y_{n-1}(0) = 0$.

Another way is to solve the equation using Fourier transform. Equation (6.47) becomes

$$\hat{y}_{n-1}(\omega)(1 + i\omega) = \hat{y}_n(\omega) \quad (6.49)$$

where $\hat{y}_n(\omega) \equiv \mathcal{F}[y_n(t)]$.

From this, implementing a coefficient C in order to impose the initial condition on $y_n(t)$,

$$\hat{y}_{n-1}(\omega) = \frac{1}{1 + i\omega} \hat{y}_n(\omega) + C\delta(\omega - i) \quad (6.50)$$

where the last term is due to the fact that $\omega = i$ is a singularity.

The Fourier transform of $y_n(t)$ in this case is

$$\mathcal{F}[k \sin(\nu t)](\omega) = ik\pi[\delta(\omega + \nu) - \delta(\omega - \nu)]. \quad (6.51)$$

Therefore

$$\begin{aligned} y_{n-1}(t) &= \frac{1}{2\pi} \int d\omega e^{i\omega t} \cdot \left[\frac{1}{1 + i\omega} \cdot ik\pi[\delta(\omega + \nu) - \delta(\omega - \nu)] + C\delta(\omega - i) \right] \\ &= \frac{e^{-i\nu t}}{2\pi} \cdot \frac{1}{1 - i\nu} ik\pi - \frac{e^{i\nu t}}{2\pi} \frac{1}{1 + i\nu} ik\pi + \frac{C}{2\pi} e^{-t} \\ &= \frac{k [\sin(\nu t) - \nu \cos(\nu t)]}{1 + \nu^2} + \frac{C}{2\pi} e^{-t} \end{aligned} \quad (6.52)$$

Imposing the i.c. $y_{n-1}(0) = 0$, $\frac{C}{2\pi} = \frac{k\nu}{1 + \nu^2}$ and so

$$y_n(t) = \frac{k}{1 + \nu^2} [\sin(\nu t) - \nu \cos(\nu t) + \nu e^{-t}] \quad (6.53)$$

that is equivalent to 6.48.

The third method is by using Laplace transforms. In this case equation (6.47) becomes

$$\mathcal{L}\{y_{n-1}(t)\}(s) = \frac{\mathcal{L}\{y_n(t)\}(s) + y_{n-1}(0)}{s + 1} \quad (6.54)$$

where the initial condition is already implemented in the formula.

Using the fact that $y_n(0) = 0$ and $\mathcal{L}\{\sin(\nu t)\}(s) = \frac{\nu}{s^2 + \nu^2}$,

$$\hat{y}_{n-1}(s) = \frac{k}{s + 1} \cdot \frac{\nu}{s^2 + \nu^2}. \quad (6.55)$$

where this time $\hat{y}_{n-1}(s) = \mathcal{L}\{y_{n-1}(t)\}(s)$.

In order to compute the inverse Laplace transform the residuals at the singularities of the function $\hat{y}_{n-1}(s)e^{st}$ have to be calculated. Indeed, the inverse Laplace transform $f(t) = \mathcal{L}^{-1}\{F(s)\}(t)$ is defined as

$$f(t) = \mathcal{L}^{-1}\{F(s)\}(t) = \frac{1}{2\pi i} \lim_{T \rightarrow \infty} \int_{\gamma-iT}^{\gamma+iT} e^{st} F(s) ds \quad (6.56)$$

and the integral can be calculated using the Cauchy residue theorem (see for example [1]) as a contour integral and so that

$$\oint_{\gamma} f(z) dz = 2\pi i \sum \text{Res}(f, a_k) \quad (6.57)$$

where a_k are the singularities of the function.

For the function in (6.55) there are three first-order poles (-1 , $i\nu$ and $-i\nu$). Then

$$\begin{aligned} y_{n-1}(t) &= \left(\frac{k\nu}{s^2 + \nu^2} e^{st} \right)_{|s=-1} + \left(\frac{k\nu}{(s+1)(s+i\nu)} e^{st} \right)_{|s=i\nu} + \left(\frac{k\nu}{(s+1)(s-i\nu)} e^{st} \right)_{|s=-i\nu} \\ &= k\nu \left[\frac{e^{-t}}{1 + \nu^2} + \frac{e^{i\nu t}}{(1+i\nu)(2i\nu)} + \frac{e^{-i\nu t}}{(1-i\nu)(-2i\nu)} \right] \\ &= k\nu \left[\frac{e^{-t}}{1 + \nu^2} + \frac{e^{i\nu t}(1-i\nu) - e^{-i\nu t}(1+i\nu)}{2i\nu(1 + \nu^2)} \right] \\ &= k\nu \left[\frac{e^{-t}}{1 + \nu^2} + \frac{2i \sin(\nu t) - 2i\nu \cos(\nu t)}{2i\nu(1 + \nu^2)} \right] \end{aligned} \quad (6.58)$$

And so at the end

$$y_{n-1}(t) = \frac{k}{1 + \nu^2} [\nu e^{-t} + \sin(\nu t) - \nu \cos(\nu t)] \quad (6.59)$$

which again is equivalent to both 6.48 and 6.53.

The three methods are equivalent but the one that seems the simplest to iterate (also because the i.c. are immediately specified) is the latter.

Indeed, using Laplace transforms, we can easily iterate the computation and write

$$\hat{y}_{n-m}(s) = \frac{k}{(s+1)^m} \cdot \frac{\nu}{s^2 + \nu^2} \quad (6.60)$$

where, for all $y_\alpha(t)$, $y_\alpha(0) = 0$.

Again, in order to anti-transform such an expression, the residuals of $e^{st} \hat{y}_{n-m}(s)$ have to be computed. This time there are two first-order poles ($i\nu$ and $-i\nu$) and the singularity $s = -1$ that is a pole of order m .

Using the definition of residuals

$$y_{n-m}(t) = \frac{1}{(m-1)!} \lim_{s \rightarrow -1} \frac{d^{m-1}}{ds^{m-1}} \left[\frac{k\nu e^{st}}{s^2 + \nu^2} \right] + k\nu \left[\frac{e^{i\nu t}}{(1+i\nu)^m} \frac{1}{2i\nu} + \frac{e^{-i\nu t}}{(1-i\nu)^m} \frac{1}{-2i\nu} \right] \quad (6.61)$$

Let us concentrate on the second term.

$$\text{Second term} = k\nu \left[\frac{e^{i\nu t}}{(1+i\nu)^m} \frac{1}{2i\nu} + \frac{e^{-i\nu t}}{(1-i\nu)^m} \frac{1}{-2i\nu} \right] = k \frac{e^{i\nu t}(1-i\nu)^m - e^{-i\nu t}(1+i\nu)^m}{(1+\nu^2)^m \cdot 2i} \quad (6.62)$$

Rewriting in the exponential form

$$1 - i\nu = (1 + \nu^2)^{1/2} e^{-i \arctan \nu} \quad 1 + i\nu = (1 + \nu^2)^{1/2} e^{i \arctan \nu} \quad (6.63)$$

$$\begin{aligned} \text{Second term} &= k \frac{(e^{i\nu t} \cdot e^{-im \arctan \nu} - e^{-i\nu t} \cdot e^{im \arctan \nu})}{(1 + \nu^2)^{\frac{m}{2}} 2i} \\ &= \frac{k \cdot \sin[\nu t - m \arctan \nu]}{(1 + \nu^2)^{\frac{m}{2}}} \end{aligned} \quad (6.64)$$

So, at the end,

$$y_{n-m}(t) = \frac{1}{(m-1)!} \lim_{s \rightarrow -1} \frac{d^{m-1}}{ds^{m-1}} \left[\frac{k\nu e^{st}}{s^2 + \nu^2} \right] + \frac{k \cdot \sin[\nu t - m \arctan \nu]}{(1 + \nu^2)^{\frac{m}{2}}}. \quad (6.65)$$

In figure 6.8 is represented the evolution of the perturbations for the first four probes using equation (6.65). Proceeding with other probes the perturbation gets smaller and smaller.

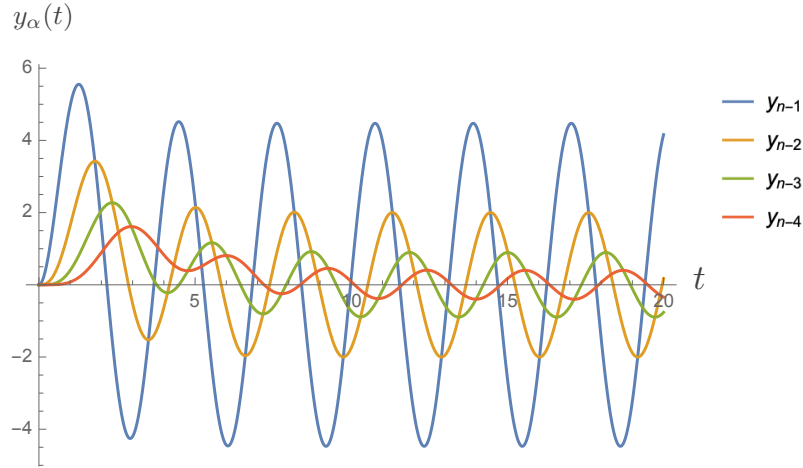


Figure 6.8: $y_\alpha(t)$ vs t .

Equation (6.65) consists of two terms. Let us try to analyse such terms separately.

The first term consists of a derivative in s of order $m-1$. It is clear that the presence of e^{st} inside the derivative (and the limit $s \rightarrow -1$) tells us

that, set finite ν and m , all the terms obtained after the derivation will be exponentially damped for large times and in particular will go to zero for $t \rightarrow \infty$.

Let us now analyse better the terms that come from the $(m-1)$ -th derivative (we'll name them T_{mrp}) in order to understand when they reach a maximum and of which order is such a value.

All the terms T_{mrp} will be of the form

$$T_{mrp} = k t^{m-1-r} e^{-t} \frac{\nu}{(1+\nu^2)^p} \frac{1}{(m-1)!} \quad (6.66)$$

for different values of r and p , considering that $r, p \in \mathbb{N}$ with $0 \leq r < m-1$ and $p > 0$.

First of all let us notice that $\frac{\nu}{(1+\nu^2)^p}$ is always less than 1. This means that

$$T_{mrp} < k t^{m-1-r} e^{-t} \frac{1}{(m-1)!} \quad (6.67)$$

The maximum of $t^{m-1-r} e^{-t} \frac{1}{(m-1)!}$ is at $t = m-1-r$ where the function has the value $(m-1-r)^{m-1-r} e^{-(m-1-r)} \frac{1}{(m-1)!}$ that, defining $q \equiv m-1-r$, can be rewritten as

$$q^q e^{-q} \frac{1}{(q+r)!} \quad (6.68)$$

The maximum of (6.68) in r is for $r = 0$, that is $q^q e^{-q} \frac{1}{q!}$. The latter is a controlled function in the sense that it does not assume very big values.

Indeed, for small q (that is always > 0) q^q it is not very big (and it is damped by the factorial and by e^{-q}) and for large q the exponential damping and the factorial *win* over q^q . This can be demonstrated for example for q large enough such that we can use Stirling approximation, for which

$$q! \sim \sqrt{2\pi q} \left(\frac{q}{e}\right)^q \quad (6.69)$$

Inserting this in (6.68) for $r = 0$ the result is

$$q^q e^{-q} \frac{1}{q!} \sim q^q e^{-q} \frac{e^q}{\sqrt{2\pi q} q^q} = \frac{1}{\sqrt{2\pi q}}. \quad (6.70)$$

This means that

$$T_{mrp} \ll k \quad (6.71)$$

and that the sum of the terms T_{mrp} will not be very large for any time t .

After this analysis of the first term of (6.65) there is still the second term to study. This time everything is simpler as the second term is just an oscillating function, a sinusoidal which maximum value is $\frac{k}{(1+\nu^2)^{\frac{m}{2}}}$.

In summary, equation (6.65) shows how the perturbation from the n -th probe propagates to the other probes.

Due to the presence of an exponential damping in the first term of (6.65), the sinusoidal part of the equation represents quite well the trend of the perturbation on the $(n - m)$ -th probe. The contribution of the first term can instead be neglected. Indeed such term is relevant just in some time interval around $t \sim m$ and also when it is relevant it assumes very small values compared to k .

At the end we can say that the propagation of the signal to probe $n - m$ is well represented by the function

$$y_{n-m}(t) = \frac{k \cdot \sin [\nu t - m \arctan \nu]}{(1 + \nu^2)^{\frac{m}{2}}} \quad (6.72)$$

and the amplitude of such a signal goes like

$$A(k, \nu, m) = \frac{k}{(1 + \nu^2)^{\frac{m}{2}}} \quad (6.73)$$

where k is just the amplitude of the initial perturbation on the n -th probe (see eq. (6.46)).

Then equation (6.73) gives the desired perturbation damping relation with distance (m) and frequency (ν).

Conclusions

In this thesis work we have studied a system of probes in a ring, locally interacting with driven colloids. In the first chapters the model has been studied for a finite system, whereas in the second part the thermodynamic limit has been analysed.

Summing up the main results and achievements:

- We found an explicit expression for the effective forces between the probes that break the action-reaction principle. These particular forces characterize the configuration as a nonequilibrium system.
- The dynamics of the probes near the crystal configuration has been found to be well modeled by a very simple differential equation in which the variables are the displacements of each probe from the equidistant configuration.
- From the dynamics' differential equation we derived an explicit solution for the displacements from the equidistant configuration. The solution has been plotted for different initial conditions and proved to generate a relaxation to a crystal pattern configuration. Such a relaxation has also been described by a compound Poisson process.
- For the crystal configuration we studied the mechanical stability using Lyapunov theory and the thermal stability by adding thermal noise to the linearized dynamics equation.
- The thermodynamic limit of the equidistant configuration has been finally analysed. We studied how a perturbation can influence and possibly break a hypothetic infinite crystal pattern. In particular we found an exponential damping relation for the perturbation inside the crystal depending on the frequency and the distance of an initial sinusoidal perturbation.

Bibliography

- [1] L. Ahlfors. *Complex Analysis: An Introduction to the Theory of Analytic Functions of One Complex Variable*. International series in pure and applied mathematics. McGraw-Hill, 1966. ISBN 9780070006560. URL <https://books.google.it/books?id=Do0uAAAAIAAJ>.
- [2] C.-Y. Chao. Circulant matrices. *SIAM Review*, 24(3):356, 1982.
- [3] M. Cross and H. Greenside. *Pattern formation and dynamics in nonequilibrium systems*. Cambridge University Press, 2009.
- [4] M. C. Cross and P. C. Hohenberg. Pattern formation outside of equilibrium. *Rev. Mod. Phys.*, 65:851–1112, Jul 1993. doi: 10.1103/RevModPhys.65.851. URL <https://link.aps.org/doi/10.1103/RevModPhys.65.851>.
- [5] J. W. Gibbs. *Elementary Principles in Statistical Mechanics: Developed with Especial Reference to the Rational Foundation of Thermodynamics*. Cambridge Library Collection - Mathematics. Cambridge University Press, 2010. doi: 10.1017/CBO9780511686948.
- [6] D. S. Goldobin and A. Pikovsky. Synchronization of self-sustained oscillators by common white noise. *Physica A: Statistical Mechanics and its Applications*, 351(1):126–132, 2005.
- [7] A. Gut. *An Intermediate Course in Probability*. Springer-Verlag New York, 01 2009. ISBN 978-1-4419-0161-3. doi: 10.1007/978-1-4419-0162-0.
- [8] P. Hartman. *Ordinary Differential Equations: Second Edition*. Classics in Applied Mathematics. Society for Industrial and Applied Mathematics (SIAM, 3600 Market Street, Floor 6, Philadelphia, PA 19104), 1982. ISBN 9780898719222. URL <https://books.google.it/books?id=NEkkJ9309okC>.
- [9] D. Jou, G. Lebon, M. Mongiovi, and R. Peruzza. Entropy flux in non-equilibrium thermodynamics. *Physica A: Statistical Mechanics and its Applications*, 338(3):445–457, 2004. ISSN 0378-4371. doi: <https://doi>.

- org/10.1016/j.physa.2004.02.011. URL <https://www.sciencedirect.com/science/article/pii/S0378437104002092>.
- [10] J. F. C. Kingman. *Poisson processes*, volume 3 of *Oxford Studies in Probability*. The Clarendon Press Oxford University Press, New York, 1993. ISBN 0-19-853693-3. Oxford Science Publications.
- [11] C. Maes and K. Netocny. Non-reactive forces and pattern formation induced by a nonequilibrium medium, 2017.
- [12] C. Maes and K. Netocny. Nonequilibrium relaxation and pattern formation. *Moscow Mathematical Journal*, 20(4):741–747, 2020. ISSN 1609-3321.
- [13] R. Martinez-Garcia. Nonequilibrium statistical physics in ecology: Vegetation patterns, animal mobility and temporal fluctuations, 2017.
- [14] R. B. Nelsen. Titu’s lemma. *Mathematics Magazine*, 93(1):70–70, 2020. doi: 10.1080/0025570X.2020.1682745. URL <https://doi.org/10.1080/0025570X.2020.1682745>.
- [15] S. Sastry. *Lyapunov Stability Theory*, pages 182–234. Springer New York, New York, NY, 1999. ISBN 978-1-4757-3108-8. doi: 10.1007/978-1-4757-3108-8-5.
- [16] T. Sekimura, S. Noji, N. Ueno, and P. Maini. *Morphogenesis and pattern formation in biological systems: experiments and models*. Springer Science & Business Media, 2013.
- [17] T. H. Tan, A. Mietke, H. Higinbotham, J. Li, Y. Chen, P. J. Foster, S. Gokhale, J. Dunkel, and N. Fakhri. Development drives dynamics of living chiral crystals, 2021.
- [18] T. Taniguchi and E. Cohen. Onsager-machlup theory for nonequilibrium steady states and fluctuation theorems. *Journal of Statistical Physics*, 126(1):1–41, 2007.
- [19] R. C. Tolman. *The principles of statistical mechanics*. Courier Corporation, 1979.
- [20] N. Weiss, P. Holmes, and M. Hardy. *A Course in Probability*. Pearson Addison Wesley, 2006. ISBN 9780201774719. URL <https://books.google.it/books?id=Be9fJwAACAAJ>.